UCRL-16419

University of California

Ernest O. Lawrence Radiation Laboratory

NUCLEAR MAGNETIC MOMENTS AND HYPERFINE ANOMALIES OF Re^{186}, Re^{188} AND Am^{241}, Am^{242}

TWO-WEEK LOAN COPY

This is a Library Circulating Copy which may be borrowed for two weeks. For a personal retention copy, call Tech. Info. Division, Ext. 5545

DISCLAIMER

This document was prepared as an account of work sponsored by the United States Government. While this document is believed to contain correct information, neither the United States Government nor any agency thereof, nor the Regents of the University of California, nor any of their employees, makes any warranty, express or implied, or assumes any legal responsibility for the accuracy, completeness, or usefulness of any information, apparatus, product, or process disclosed, or represents that its use would not infringe privately owned rights. Reference herein to any specific commercial product, process, or service by its trade name, trademark, manufacturer, or otherwise, does not necessarily constitute or imply its endorsement, recommendation, or favoring by the United States Government or any agency thereof, or the Regents of the University of California. The views and opinions of authors expressed herein do not necessarily state or reflect those of the United States Government or any agency thereof or the Regents of the University of California.

UCRL-16419

UNIVERSITY OF CALIFORNIA

Lawrence Radiation Laboratory
Berkeley, California

AEC Contract No. W-7405-eng-48

NUCLEAR MAGNETIC MOMENTS AND HYPERFINE ANOMALIES OF Re^{186}, Re^{188} AND Am^{241}, Am^{242}

Lloyd Armstrong, Jr.

(Ph. D. Thesis)

September 23, 1965

NUCLEAR MAGNETIC MOMENTS AND
HYPERFINE ANOMALIES OF Re^{186}, Re^{188} AND Am^{241}, Am^{242}

Contents

Abstract iii

I. Introduction 1

II. Theory

A. Fine Structure 2

B. Hyperfine Structure

1. Nonrelativistic Treatment 5

2. Relativistic Treatment 11

C. Second-Order Effects 23

D. Exchange Polarization 25

E. Hyperfine Anomalies 28

F. Collective Model of the Nucleus 31

III. Experimental Method 37

IV. Apparatus 42

V. Rhenium

A. Introduction 46

B. Experimental Method and Results 46

C. Second-Order Effects 51

D. Hyperfine Fields 53

E. Nuclear Structure 63

VI. Americium

A. Introduction 66

B. Experimental Methods and Results 66

C. Second-Order Effects 72

D. Hyperfine Fields 73

E. Nuclear Structure 84

Acknowledgments 88

References 89

NUCLEAR MAGNETIC MOMENTS AND HYPERFINE ANOMALIES OF Re^{186}, Re^{188} AND Am^{241}, Am^{242}

Lloyd Armstrong, Jr.

Lawrence Radiation Laboratory
University of California
Berkeley, California

ABSTRACT

The method of triple resonance in an atomic beam has been used to measure the nuclear moments of two isotopes each of rhenium and americium. These moments were found to be

$$\mu_I(Re^{186}) = +1.728(0.003) \text{ nm}$$

$$\mu_I(Re^{188}) = +1.777(0.005) \text{ nm}$$

$$\mu_I(Am^{241}) = +1.58(0.03) \text{ nm}$$

$$\mu_I(Am^{242}) = +0.3808(0.0015) \text{ nm.}$$

All values were corrected for diamagnetic shielding. These values of the moments lead to anomalies of

$$^{186}\Delta^{188} = +0.1(0.4)\%$$

for Re, and

$$^{241}\Delta^{242} = +1.7(2.0)\%$$

for Am.

In addition, the hyperfine structures of Re and Am were calculated relativistically. It was found that relativistic effects alone explain the hyperfine structure of Re, but that both relativistic effects and core polarization are needed to explain the hyperfine structure of Am.

The nuclear moments of Re and Am were analyzed by means of the Nilsson model. Excellent agreement was found between theorical and experimental values with the use of quenched g factors.

I. INTRODUCTION

This paper describes measurements of nuclear magnetic moments made on two rhenium and two americium isotopes. These four isotopes have much in common: Both Re and Am have electronic ground states with zero orbital angular momentum, and all four isotopes lie in regions best described by the collective model.

The measurements were all made by the method of triple resonance in an atomic beam. Prior to this work, this method had been used on stable isotopes only. These measurements showed that the technique was efficient enough to be used on beams of radioactive nuclei, which are generally very much less intense than beams of stable nuclei.

This paper also describes in detail two methods of calculating relativistic hyperfine structures. The part of this work concerning Re has already been published;[1] this Re paper was one of the first in which relativistic effects in heavy atoms were considered, and the importance of the effect was clearly shown.

II. THEORY

A. Fine Structure

The nonrelativistic Hamiltonian for a noninteracting atom in a field-free region is given to a good approximation by

$$\mathcal{H} = \sum_{i=1}^{N} \left[\frac{p_i^2}{2m} - \frac{Ze^2}{r_i} + \zeta(r_i)\, \ell_i \cdot s_i + \sum_{i>j} \frac{e^2}{r_{ij}} \right] + \mathcal{H}_{hfs}. \tag{1}$$

In this expression, r_i is the distance from a (point) nucleus to the ith electron, r_{ij} is the distance between the ith and jth electrons, and $\zeta(r_i)\, \ell_i \cdot s_i$ is the interaction energy of the spin dipole moment of the ith electron with the field produced by its own orbital motion. There are also contributions to $\mathcal{H}$ from the interaction of the orbital motions of two electrons, the interaction of the spins of two electrons, and interactions between the spin of one electron and the orbit of another; these contributions are small and are usually neglected.

The expression in brackets represents the interaction of orbital electrons with a point nucleus, and gives rise to the atomic fine structure. The term $\mathcal{H}_{hfs}$, the hyperfine-structure Hamiltonian, contains the corrections necessary to explain the interaction of the orbital electrons with a nucleus having a finite volume. This term is much smaller than the fine-structure Hamiltonian and can be considered a perturbation.

As the fine-structure Hamiltonian is itself too complicated to allow an exact solution, the usual procedure is to solve instead the equation

$$\mathcal{H}' = \sum_{i} \frac{p_i^2}{2m} + U(r_i). \tag{2}$$

Here $U(r_i)$ is the spherically symmetric average of the other charges at the position of the ith electron. For good choices of $U(r_i)$, the remaining term $V = \mathcal{H} - \mathcal{H}'$ will be small and can be treated by perturbation theory. Not only is $\mathcal{H}'$ separable into parts containing only the coordinates of a single electron, but these parts are further separable into radial and angular parts. The wave function that is a

solution to $\mathcal{H}'\psi = E'\psi$ can therefore be given by a product of single-particle wave functions, each having the form

$$\psi_i = R_i(n\ell)Y_m^{\ell}(\theta_i\phi_i) \tag{3}$$

(but see Sec. II. D).

For light atoms, $e^2/r_{ij} >> \xi(r_i)\ell_i \cdot s_i$, and the latter term can be considered a perturbation. We can define $S = \sum_i s_i$ and $L = \sum_i \ell_i$, the total spin and orbital angular momenta. Since e^2/r_{ij} does not depend on the particle spin coordinates, S and e^2/r_{ij} obviously commute. Consideration of the action of a typical component L on $\sum_{i>j} e^2/r_{ij}$, e.g.,

$$L_x \sum_{i>j} e^2/r_{ij} =$$

$$\frac{1}{i}\sum_i \left(y_i \frac{\partial}{\partial z_i} - z_i \frac{\partial}{\partial y_i}\right) e^2 \sum_{i>j}\left[\frac{1}{(x_i-x_j)^2+(y_i-y_j)^2+(z_i-z_j)^2}\right]^{1/2}$$

$$= \sum_{i>j}\left\{e^2/r_{ij}\, L_x\right\} \tag{4}$$

shows that L also commutes with $\sum_{i>j} e^2/r_{ij}$, making both L and S "good" quantum numbers to a high degree of accuracy. Because $\mathcal{H}$ is spherically symmetric, its eigenvalues cannot depend on M_L or M_S, but only on L and S. The eigenvalues of $\mathcal{H}$ are therefore $(2\ell+1)(2s+1)$-fold degenerate; the corresponding eigenstates comprise a term. The perturbing term $\sum_i \xi(r_i)\ell_i \cdot s_i$ does not commute with either L or S, but does with their vector sum $\vec{J} = \vec{L} + \vec{S}$. This latter statement can be easily verified by looking at the commutator of any component of J with $\ell_i \cdot s_i$, e.g.,

$$\left[J_x, \ell_i \cdot s_i\right] = \left[\sum_{k \neq i} j_{kx}, \ell_i \cdot s_i\right] + \left[j_{ix}, \ell_i \cdot s_i\right] =$$

$$\left[s_{ix} + \ell_{ix}, \ell_{ix} s_{ix} + \ell_{iy} s_{iy} + \ell_{iz} s_{iz}\right] = 0. \tag{5}$$

The perturbation $\sum_i \xi(r_i) \ell_i \cdot s_i$ therefore splits a term into multiplets of degeneracy 2J+1 labeled by L, S, and J. This coupling scheme is called LS or Russell-Saunders coupling.

At the opposite extreme, $\sum_i \xi(r_i) \ell_i \cdot s_i >> \sum_{i>j} e^2/r_{ij}$, and the ℓ and s values for each electron couple to a j value, with the j's then coupling to J, i.e., $\vec{J} = \sum_i \vec{j}_i$. This is called j-j coupling.

In most actual situations, neither LS nor j-j coupling can completely explain the results. That is, neither e^2/r_{ij} nor $\xi(r_i)\ell_i \cdot s_i$ is overwhelmingly larger than the other, and L, S, and j can no longer commute with the Hamiltonian. J, however, is a good quantum number, since it commutes with both perturbation terms.

Addition of an external magnetic field destroys the spherical symmetry of the atomic environment, replacing it with a two-dimensional symmetry. The atomic states must therefore transform according to R2, and be labeled by projection values along the direction of the magnetic field (z direction). Because R2 has only one-dimensional representations, the degeneracy of the eigenvalues is completely lifted.

The interaction of an atom with an external field is described by the Hamiltonian

$$\mathcal{H}^1_{ext} = -\mu_0 \, (L + g_S) \cdot H \quad . \tag{6}$$

The term $\mathcal{H}^1_{ext}$ is not diagonal in the $LSJM_J$ system, but is in the LM_LSM_S system. For small values of H, however, the spin-orbit interaction dominates (for the LS coupling case), and L and S still couple to J to a high degree of accuracy. In this case

$$\left\langle LSJM_J \right| -\mu_0(L_z + g_S)H_z \left| LSJM_J \right\rangle = -\mu_0 \left[\frac{J(J+1) + L(L+1) - S(S+1)}{2J(J+1)} \right.$$

$$\left. + \; g_S \; \frac{J(J+1) + S(S+1) - L(L+1)}{2J(J+1)} \right] M_J H_z$$

$$= - g_J \mu_0 H_z M_J \, . \tag{7}$$

B. Hyperfine Structure

1. Nonrelativistic Treatment

Thus far we have neglected the effects of the nucleus on the fine structure, i.e., $\mathcal{H}_{hfs}$. As mentioned above, these effects are due to the finite size of the nucleus. For instance, if the nucleus is not a point charge at the origin, we must express the Coulomb interaction between an electron and the nucleus as an integral over volume elements of the electron and the nucleus, i.e.,

$$\left\langle \mathcal{H}_E \right\rangle = \int_{\tau_e} \int_{\tau_n} \frac{\rho_e \rho_n}{|r_e - r_n|} \, d\tau_e d\tau_n, \tag{8}$$

where $\rho_e = -e\psi^*(e)\psi(e)$, $\rho_n = e\psi^*(n)\psi(n)$. If we assume that $r_e > r_n$, expand $1/r$ in terms of Legendre polynomials, and use the spherical harmonic addition theorem, this becomes

$$\left\langle \mathcal{H}_E \right\rangle = \sum_K \sum_m (-1)^m \left[\int_{\tau_e} \sqrt{\frac{4\pi}{2K+1}} \; \frac{\rho_e}{r_e^{K+1}} \; Y^K_{-m} \, (\theta_e \phi_e) d\tau_e \right]$$

$$\times \left[\int_{\tau_n} \sqrt{\frac{4\pi}{2K+1}} \; \rho_n \; r_n^K \; Y^K_m (\theta_n \phi_n) \, d\tau_n \right] \tag{9}$$

or

$$\mathcal{H}_E = \sum_K Q^K(e) \cdot F^K(n) . \tag{10}$$

The terms Q^K and F^K are spherical tensor operators of rank K operating on the electronic and nuclear coordinates, respectively. Comparison of (9) and (10) shows that they are given by

$$Q^K_m = - \sqrt{\frac{4\pi}{2K+1}} \frac{e}{r_e^{K+1}} Y^K_m (\theta_e \phi_e) \tag{11a}$$

and

$$F^K_m = e \sqrt{\frac{4\pi}{2K+1}} r_n^K Y^K_m(\theta_n \phi_n). \tag{11b}$$

If we consider only stationary nuclear and electric-current distributions, that is, $\nabla \cdot j = 0$, then we can write

$$j_n = c\nabla_n \times M_n \tag{12a}$$

and

$$j_e = c\nabla_e \times M_e . \tag{12b}$$

Here M_e and M_n are, like B and H, pseudovectors. Ramsey has shown that under these conditions we can write the magnetic interaction[2]

$$\langle \mathcal{H}_M \rangle = + \frac{1}{2c} \int A_e \cdot j_n \, d\tau$$

as:

$$\langle \mathcal{H}_M \rangle = \iint \frac{\nabla_e \cdot M_e \; \nabla_n \cdot M_n}{|r_e - r_n|} \, d\tau_e \, d\tau_n . \tag{13}$$

This has the same form as (8); by the same procedure used in treating the Coulomb interaction we obtain

$$\mathcal{H}_M = \sum_K M^K(e) \cdot N^K(n) \tag{14}$$

where

$$M_m^K = \sqrt{\frac{4\pi}{2K+1}} \; \frac{\nabla_e \cdot M_e}{r_e^{K+1}} \; Y_m^K(\theta_e \phi_e) \tag{15a}$$

and

$$N_m^K = \sqrt{\frac{4\pi}{2K+1}} \; (\nabla_n \cdot M_n) \, r_n^K \; Y_m^K(\theta_n \phi_n). \tag{15b}$$

The perturbing term $\mathcal{H}_{hfs} = \mathcal{H}_M + \mathcal{H}_E$ does not commute with either J or I, the nuclear spin, but does with their vector sum F. This statement can be proved by considering the effect of any component of F on the term

$$\sum_m (-1)^m \; Y_m^K(\theta_e \phi_e) \; Y_{-m}^K(\theta_n \phi_n),$$

i.e.,

$$\begin{aligned} F_x \sum_m (-1)^m \; & Y_m^K(\theta_e \phi_e) \; Y_{-m}^K(\theta_n \phi_n) \\ &= (F_+ + F_-) \sum_m (-1)^m \; Y_m^K(\theta_e \phi_e) \; Y_{-m}^K(\theta_n \phi_n) \\ &= (J_+ + I_+ + J_- + I_-) \sum_m (-1)^m \; Y_m^K(\theta_e \phi_e) \; Y_{-m}^K(\theta_n \phi_n) \\ &= \left[\sum_m (-1)^m \; Y_m^K(\theta_e \phi_e) \; Y_{-m}^K(\theta_n \phi_n) \right] F_x . \end{aligned} \tag{16}$$

The 2J+1 degenerate fine-structure levels are therefore split into 2I+1 or 2J+1 (whichever number is smaller) levels by the hyperfine-structure interaction. The new levels are 2F+1 degenerate in the absence of an external field.

The interaction of the nucleus with an external field is given by $\mathcal{H}^2_{ext} = -g_I\mu_0 I\cdot H = -\mu_I\cdot H$. The total interaction of the atom with an external magnetic field is then given by $\mathcal{H}_{ext} = \mathcal{H}^1_{ext} + \mathcal{H}^2_{ext} = -g_J\mu_0 J\cdot H - g_I\mu_0 I\cdot H$. This term does not commute with F, but as in the fine-structure case, F is an approximately good quantum number at low fields. Therefore, at low fields the effect of the magnetic field is to remove the 2F+1 degeneracy of the eigenvalues through the interaction

$$\left\langle IJFM \middle| \mathcal{H}_{ext} \middle| IJFM \right\rangle = -g_F\mu_0 HM \tag{17}$$

where

$$g_F = g_J \frac{F(F+1) + J(J+1) - I(I+1)}{2F(F+1)} + g_I \frac{F(F+1) + I(I+1) - J(J+1)}{2F(F+1)} .$$

In the high-field region (nuclear Paschen-Back), F is no longer a good quantum number and eigenstates are best labeled by IM_IJM_J.

Matrix elements of operators having the form of (10) and (14) are easily taken in a representation where I and J couple to F [(IJFM) representation]:

$$\sum_K \left\langle IJFM \middle| Q^K\cdot F^K \middle| I'J'F'M' \right\rangle = \sum_K (-1)^{I'+J+F} \delta_{FF'}\delta_{MM'}$$

$$\times \begin{Bmatrix} I & J & F \\ J' & I' & K \end{Bmatrix} \left\langle J \,||Q||\, J' \right\rangle \left\langle I \,||F||\, I' \right\rangle . \tag{18}$$

The 6j symbol shows that the series breaks off for either $J + J' < K$ or $I + I' < K$.

The total Hamiltonian $\mathcal{H}_T = \mathcal{H} + \mathcal{H}_{ext}$ is invariant under π, the parity operator, and therefore the eigenvectors of $\mathcal{H}$ must also be eigenvectors of π. In addition, $\left\langle \psi \middle| \theta \middle| \psi \right\rangle$ must have positive parity, since integrals over all space cannot depend on axis inversion. Because ψ has a definite parity, ψ^2 will have positive parity; θ must therefore have positive parity for $\left\langle \psi \middle| \theta \middle| \psi \right\rangle$ to be nonzero.

Operators Q^K and F^K both have the parity of Y^K, that is, $(-1)^K$. Therefore, only K even values are allowed in the electric case. Since $M_e(M_n)$ is a pseudovector, $\nabla \cdot M_e(\nabla \cdot M_n)$ is a pseudoscalar having parity -1, and M^K and N^K have the parity of $(-1)Y^K$, or $(-1)^{K+1}$. Therefore, only K odd values are allowed in the magnetic case.

The first allowed electric interaction is $Q^0 \cdot F^0$, which is exactly the Coulomb term given in (1). The second allowed term is $Q^2 \cdot F^2$, the electric quadrupole term. By defining

$$Q = (2/e) \left\langle II \middle| Q_0^2 \middle| II \right\rangle \tag{19a}$$

$$q_J = -(2/e) \left\langle JJ \middle| F_0^2 \middle| JJ \right\rangle \tag{19b}$$

and using (18), one obtains

$$\left\langle IJFM \middle| Q^2 \cdot F^2 \middle| IJFM \right\rangle = \frac{-e^2 q_J Q \left[3K(K+1) - 4I(I+1)J(J+1) \right]}{8IJ(2I-1)(2J-1)} , \tag{20}$$

where $K = F(F+1) - I(I+1) - J(J+1)$.

The term Q is, of course, the nuclear quadrupole moment (or $\frac{1}{e}Q_{33}$), and q_J is the gradient of the z component of the electric field at the origin, $+\left\langle \partial E_z / \partial z \right\rangle$. One generally defines

$$B = -e^2 q_J Q. \tag{21}$$

The first allowed magnetic interaction is $M^1 \cdot N^1$. Consideration of the classical interpretation of M^1 and N^1 shows that

$$\left\langle JJ \middle| M_0^1 \middle| JJ \right\rangle = \int \frac{\nabla_e \cdot m_e \cos\theta}{r_e^2} \, d\tau_e = \frac{1}{c} \int \frac{[j_e \times (-r_e)]_z}{r_e^3} \, d\tau_e$$

$$= - [B_J(0)]_z , \tag{22}$$

and

$$\left\langle II \middle| N_0^1 \middle| II \right\rangle = \frac{1}{2c} \int (r \times j_n)_z \, d\tau_n = (\mu_I)_z . \tag{23}$$

Using (18), (22), and (23), we can then write

$$\left\langle IJFM \middle| M^1 \cdot N^1 \middle| IJFM \right\rangle = - \frac{\mu_I B_z}{IJ} \, I \cdot J \, . \tag{24}$$

One generally defines the magnetic dipole constant A as

$$A = - \frac{\mu_I B_z}{IJ} \quad . \tag{25}$$

An expression for the magnetic field at the nucleus can easily be derived for a single nonrelativistic electron in a central field. The magnetic field due to an electron with position $\vec{r}$, velocity $\vec{v}$, and angular momentum $\vec{\ell}$ is

$$\vec{B}_\ell = - e \frac{\vec{v} \times (-\vec{r})}{c r^3} = - \frac{e\hbar}{mc} \frac{\vec{\ell}}{r^3} = -2 \mu_0 \frac{\vec{\ell}}{r^3} \quad .$$

The field due to a dipole is

$$\vec{B}_S = - \frac{1}{r^3} \left(\vec{\mu} - \frac{3\vec{\mu} \cdot \vec{r}}{r^2} \vec{r} \right) = \frac{2\mu_0}{r^3} \left[\vec{s} - \frac{3\vec{s} \cdot \vec{r}}{r^2} \vec{r} \right] .$$

The total field is then

$$\vec{B} = - \frac{2\mu_0}{r^3} \left[\vec{\ell} - \vec{s} + \frac{3 s \cdot r}{r^2} \vec{r} \right] . \tag{26}$$

The last term on the right can be further simplified into

$$\frac{3(s \cdot r) r}{r^2} = 3(S \cdot C^1) C^1 = -3\sqrt{3} \left[(SC^1)^0 C^1 \right]^1$$

$$= -3\sqrt{3} \sum_K \begin{Bmatrix} 1 & 1 & K \\ 1 & 1 & 0 \end{Bmatrix} \sqrt{2K+1} \, \sqrt{3} \left[(C^1 C^1)^K s \right]^1$$

$$= \vec{S} - \sqrt{10} \, (s \, C^2)^1 ,$$

where we have used in the last step

$$\left(C^{K_1} \, C^{K_2} \right)^{K_3} = (-1)^{K_3} \sqrt{2K_3+1} \begin{pmatrix} K_1 & K_2 & K_3 \\ 0 & 0 & 0 \end{pmatrix} C^{K_3}$$

The z component of (26) then becomes

$$B_z = -\frac{2\mu_0}{r^3}\left[\ell_z - \sqrt{10}\,(sC^2)^1_0\right] = -\frac{2\mu_0}{r^3}\,N_z\,. \tag{27}$$

The above discussion is valid only for the case of $r_e > r_n$; however, s electrons have large values of $|\psi|^2$ at the origin and thereby violate this restriction. This density at the origin does not affect the electric quadrupole moment, since s electrons have spherically symmetric densities and therefore cannot contribute to the quadrupole interaction. Fermi[3] showed that in the magnetic dipole interaction there was a "contact" term due to the nonspherical nature of the s electron spin densities at the nucleus:

$$A_s = \frac{16\pi}{3}\,g_I\mu_0^2\,|\psi_0|^2 \tag{28a}$$

for a single s electron. This term is derived in Sec. II. B. 2. When more than one s electron is involved, or when electrons of different ℓ's also contribute to J, the proper form for (28) is

$$A_s = \frac{16\pi}{3}\,g_I\,\frac{\mu_0^2}{J}\,\left\langle JJ\left|\sum_i s_{zi}\,\delta(r_i)\right|JJ\right\rangle\,. \tag{28b}$$

2. Relativistic Treatment

The Hamiltonian for a single relativistic electron in a central field is

$$\mathcal{H}_0(R)\psi = (\alpha\cdot cp + \beta mc^2 - eV_c)\,\psi = E\psi, \tag{29}$$

where

$$\beta = \begin{pmatrix} 1 & 0 \\ 0 & -1 \end{pmatrix}, \quad \vec{\alpha} = \begin{pmatrix} 0 & \vec{\sigma} \\ \vec{\sigma} & 0 \end{pmatrix}, \text{ and } \sigma = \text{Pauli spin matrices.}$$

This is the relativistic equivalent of (2). Here ψ is a column matrix of four rows, and can be separated into

$$\psi = \begin{pmatrix} \psi \\ \phi \end{pmatrix}, \tag{30}$$

where in the nonrelativistic limit ϕ goes to zero and ψ is the nonrelativistic wave function. Solutions to (29) are

$$\psi_{jm} = \begin{pmatrix} \psi_{\ell jm} \\ \phi_{\bar{\ell} jm} \end{pmatrix} \qquad \bar{\ell} = \ell \pm 1 \quad \text{as } j = \ell \pm 1/2$$

$$\psi_{\ell jm} = \frac{F(r)}{r} Y_{\ell jm} \tag{31}$$

$$\phi_{\ell jm} = \frac{iG(r)}{r} Y_{\ell jm},$$

where

$$Y_{\ell jm} = \sum_{m_\ell m_s} \begin{pmatrix} \ell & \frac{1}{2} & j \\ m_\ell & m_s & m \end{pmatrix} \sqrt{2J+1} \; Y^{\ell}_{m_\ell} \chi^{1/2}_{m_s} .$$

Equations for F and G can be obtained by solving (29) using (31), and then using

$$\alpha \cdot p = \alpha_r \left[p_r + \frac{i}{r(1 + \sigma \cdot L)} \right]$$

where $\alpha_r = \alpha \cdot r,$

and $(\sigma \cdot r) Y_{\ell jm} = -Y_{\bar{\ell} jm}$

$$(\sigma \cdot r) Y_{\bar{\ell} jm} = -Y_{\ell jm} .$$

This gives

$$\left(\frac{d}{dr} - \frac{K}{r} \right) F = \frac{1}{\hbar c} (mc^2 + E + eV_c) G \tag{32}$$

$$\left(\frac{d}{dr} + \frac{K}{r} \right) G = \frac{1}{\hbar c} (mc^2 - E - eV_c) F,$$

where

$$(1 + \sigma \cdot L)\psi = K\psi, \quad (1 + \sigma \cdot L)\phi = -K\phi.$$

We see from the above equations that ℓ is no longer a good quantum number for individual electrons, but that j is.

As in Sec. II. A, our perturbing Hamiltonian is given by

$$\mathcal{H}_T(R)-\mathcal{H}_0(R) = [\alpha\cdot(cp + eA) + \beta mc^2 - eV] - \mathcal{H}_0(R) = -e(V - V_c) + e\alpha\cdot A. \tag{33}$$

We see that the electronic terms, those deriving from a scalar potential, have exactly the same form in (29) as in (1). We therefore would expect that the electric quadrupole operator is the same in the relativistic as in the nonrelativistic case. The interaction with a vector potential is, however, quite different, and we should expect the operators for the magnetic moments to be changed in going from the nonrelativistic to the relativistic. Schwartz[4] has shown that $e\alpha\cdot A$ can be expanded in a series of the same form as (14). The general derivation is rather complicated, but an expression can be derived for the particular case of the dipole term.

We saw in the previous section that the nucleus has a magnetic dipole moment μ_I; this produces an A given by

$$A = \frac{\mu_I \times r}{r^3} \quad . \tag{34}$$

Since $\vec{\alpha} = \begin{pmatrix} 0 & \vec{\sigma} \\ \vec{\sigma} & 0 \end{pmatrix}$, we are interested in terms of the form $e\sigma\cdot A$

$$e\sigma\cdot A = e\sigma\cdot \frac{\mu_I\times r}{r^3} = e\mu_I\cdot \frac{r\times\sigma}{r^3}$$

$$= e\mu_I\cdot \frac{C^1\times\sigma}{r^2} = -ie\sqrt{2}\,\vec{\mu}_I\cdot \frac{(C^1\sigma)^1}{r^2}\,. \tag{35}$$

We can equate this with the nonrelativistic dipole operators

$$-\vec{\mu}_I\cdot \vec{B}_J = -\,ie\sqrt{2}\,\vec{\mu}_I\cdot \frac{(C^1\sigma)^1}{r^2}$$

or

$$\vec{B}_J = ie\sqrt{2}\,\frac{(C^1\sigma)^1}{r^2} \quad . \tag{36}$$

A typical matrix element of the dipole interaction will then be

$$\left\langle \psi_{jm} \middle| e\alpha\cdot A \middle| \psi_{j'm'} \right\rangle = \int \left(\frac{F(r)}{r} Y_{\ell jm} \middle| \left(\frac{iG(r)}{r} Y_{\bar{\ell} jm} \right) \right| \begin{vmatrix} 0 & e\sigma\cdot A \\ e\sigma\cdot A & 0 \end{vmatrix} \left(\begin{matrix} \frac{F'(r)}{r} Y_{\ell' j' m'} \\ \frac{iG'}{r} Y_{\bar{\ell}' j' m'} \end{matrix} \right)$$

$$\times \quad d\tau$$

$$= i \int \left[\frac{F(r)}{r} Y_{\ell jm} \middle| e\sigma\cdot A \middle| \frac{G'(r)}{r} Y_{\bar{\ell}' j' m'} \right] d\tau$$

$$-i \int \left[\frac{G(r)}{r} Y_{\bar{\ell} jm} \middle| e\sigma\cdot A \middle| \frac{F'(r)}{r} Y_{\ell' j' m'} \right] d\tau$$

$$= + \mu_I \sqrt{2}\, e \left\langle \ell jm \middle| (C^1\sigma)^1_0 \middle| \bar{\ell}' j' m' \right\rangle \int_0^\infty \frac{FG'}{r^2} dr$$

$$+ \mu_I \sqrt{2}\, e \left\langle \bar{\ell} jm \middle| (C^1\sigma)^1_0 \middle| \ell' j' m' \right\rangle \int_0^\infty \frac{F'G}{r^2} dr$$

$$= + \sqrt{2}\, \mu_I e (-1)^{j-m+\ell'} \begin{pmatrix} j & 1 & j' \\ -m & 0 & m' \end{pmatrix} \begin{pmatrix} j & 1 & j' \\ -\frac{1}{2} & 1 & -\frac{1}{2} \end{pmatrix} \sqrt{2j+1}\, \sqrt{2j'+1}$$

$$\times \left[\int_0^\infty \frac{FG'}{r^2} dr + \int_0^\infty \frac{F'G}{r^2} dr \right] . \qquad (37)$$

As stated above, the electric quadrupole operator is the same in the relativistic case as in the nonrelativistic. We therefore wish to evaluate

$$\left\langle \psi_{\ell jm} \middle| \frac{1}{e} \frac{2}{r^3} C_0^2 \middle| \psi_{\ell' j' m'} \right\rangle = \frac{2}{e} \left\langle \ell jm \middle| C_0^2 \middle| \ell' j' m' \right\rangle \int^{\infty} \frac{FF'}{r^3} dr$$

$$+ \frac{2}{e} \left\langle \bar{\ell} jm \middle| C_0^2 \middle| \bar{\ell}' j' m' \right\rangle \int^{\infty} \frac{GG'}{r^3} dr$$

$$= \frac{2}{e} (-1)^{j-m+j'+3/2} \begin{pmatrix} j & 2 & j' \\ -m & 0 & m' \end{pmatrix} \begin{pmatrix} j & 2 & j' \\ -\frac{1}{2} & 0 & \frac{1}{2} \end{pmatrix} \sqrt{2j+1} \sqrt{2j'+1}$$

$$\times \int^{\infty} \left(\frac{FF'}{r^3} + \frac{GG'}{r^3} \right) dr . \tag{38}$$

Many times eigenstates are expanded in terms of an $\ell m_\ell s m_s$ wave function. It is therefore of interest to calculate matrix elements in this scheme. Since ℓ is not a good quantum number, we must first expand $\ell m_\ell s m_s$ wave functions in terms of $\ell s j m_j$ wave functions.

$$\left| \ell m_\ell s m_s \right\rangle = C_1 \left| \ell \; j=\ell+\tfrac{1}{2} \; m \right\rangle + C_2 \left| \ell \; j=\ell-\tfrac{1}{2} m \right\rangle ,$$

where C_1 and C_2 are Clebsch-Gordan coefficients. For simplicity, we restrict ourselves in what follows to configurations of particles having only one angular momentum, that is, the electronic properties of the atom arise from the configuration $(\ell)^N$. Then

$$\left\langle \ell m_\ell s m_s \middle| \theta \middle| \ell m'_\ell s m'_s \right\rangle = C_1 C'_1 \left\langle \ell j_+ m \middle| \theta \middle| \ell j_+ m' \right\rangle + C_2 C'_2 \left\langle \ell j_- m \middle| \theta \middle| \ell j_- m' \right\rangle$$

$$+ C_1 C'_2 \left\langle \ell j_+ m \middle| \theta \middle| \ell j_- m' \right\rangle + C_2 C'_1 \left\langle \ell j_- m \middle| \theta \middle| \ell j_+ m' \right\rangle , \tag{39}$$

where + indicates the $(j=\ell+\frac{1}{2})$ state, - the $(j=\ell-\frac{1}{2})$ state.

We can now combine (36), (37), (38), and (39) to get

$$\left\langle \ell m_\ell s m_s \middle| B_{Jz} \middle| \ell m'_\ell s m'_s \right\rangle = C_1 C'_1 e \frac{2m(\ell+1)}{(\ell+\frac{1}{2})(\ell+\frac{3}{2})} \int_0^\infty \frac{F_+ G_+}{r^2} dr$$

$$- C_2 C'_2 e \frac{2m\ell}{(\ell-\frac{1}{2})(\ell+\frac{1}{2})} \int_0^\infty \frac{F_- G_-}{r^2} dr$$

$$-e(C_1 C'_2 + C_2 C'_1) \frac{[(\ell+m+\frac{1}{2})(\ell-m+\frac{1}{2})]^{1/2}}{(2\ell+1)} \int_0^\infty \frac{F_+ G_- + F_- G_+}{r^2} dr \tag{40}$$

and

$$\left\langle \ell m_\ell s m_s \middle| q_J \middle| \ell m_\ell s m_s \right\rangle = C_1 C'_1 \frac{1}{2} \frac{(\ell+\frac{1}{2})(\ell+\frac{3}{2}) - 3m^2}{(\ell+\frac{1}{2})(\ell+\frac{3}{2})} \int_0^\infty \frac{F_+^2 + G_+^2}{r^3} dr$$

$$+ C_2 C'_2 \frac{(\ell-\frac{1}{2})(\ell+\frac{1}{2}) - 3m^2}{(\ell-\frac{1}{2})(\ell+\frac{1}{2})} \int_0^\infty \frac{F_-^2 + G_-^2}{r^3} dr$$

$$-(C_1 C'_2 + C_2 C'_1) \frac{12m[(\ell+\frac{1}{2}+m)(\ell+\frac{1}{2}-m)]^{1/2}}{(2\ell-1)(2\ell+1)(2\ell+3)} \int_0^\infty \frac{F_+ F_- + G_+ G_-}{r^3} dr. \tag{41}$$

In many cases, configurations may be too complicated to expand in determinantal product states. In such cases, one would prefer to have the relativistic term expressed in terms of tensor operators. That is, we want

$$\left\langle j \middle| \middle| e\alpha \cdot A \middle| \middle| j' \right\rangle = \sum_{\kappa K} a_{\kappa K} \left\langle j \middle| \middle| w^{(\kappa K)1} \middle| \middle| j' \right\rangle \tag{42}$$

where

$$w^{(\kappa K)1} = (t^{\kappa} v^{K})^{1}$$

$$\left\langle \ell \,||\, v^{K} \,||\, \ell' \right\rangle = \delta(\ell\ell')\,[K]^{1/2} \tag{43}$$

$$\left\langle s \,||\, t^{\kappa} \,||\, s' \right\rangle = \delta(ss')\,[\kappa]^{1/2}.$$

Using

$$\left\langle j \,||\, w^{(\kappa K)1} \,||\, j' \right\rangle = ([j][j']3[K][\kappa])^{1/2} \tag{44}$$

$$\begin{Bmatrix} \ell & \ell & K \\ 1/2 & 1/2 & \kappa \\ j & j' & 1 \end{Bmatrix} (-1)^{\kappa+K+1}$$

and Eq. (37), we obtain

$$-\mu_I e(-1)^{\ell'} (2[j][j'])^{1/2} \begin{pmatrix} j & 1 & j' \\ -1/2 & 1 & -1/2 \end{pmatrix} \int \frac{FG' + F'G}{r^2} \, dr$$

$$= \sum a_{\kappa K} (3[j][j'][\kappa][K]^{1/2} (-1)^{\kappa+K+1} \begin{Bmatrix} \ell & \ell & K \\ 1/2 & 1/2 & \kappa \\ j & j' & 1 \end{Bmatrix} .$$

Then, multiplying both sides by

$$\sum_{jj'} \begin{Bmatrix} \ell & \ell & K' \\ 1/2 & 1/2 & \kappa' \\ j' & j & 1 \end{Bmatrix} ([j][j'][K][\kappa]^{1/2},$$

we obtain

$$a_{\kappa K} \sqrt{3}\,(-1)^{\kappa+K+1} = -\mu_I e(-1)^{\ell'} (2[K][\kappa])^{1/2} \sum_{jj'} \begin{pmatrix} j' & 1 & j \\ -1/2 & 1 & -1/2 \end{pmatrix} [j][j']$$

$$\times \begin{Bmatrix} \ell & \ell & K \\ 1/2 & 1/2 & \kappa \\ j' & j & 1 \end{Bmatrix} \int \frac{F_j G_{j'} + F_{j'} G_j}{r^2} \, dr .$$

Expanding this leads to

$$\alpha_{10} = -2\,\mu_n e \sqrt{\frac{8}{9(2\ell+1)^3}}\;\left[(\ell+1)^2 P_{++} + \ell(\ell+1)P_{+-} + \ell^2 P_{--}\right]$$

$$\alpha_{01} = +\,2\,\mu_n e \sqrt{\frac{2\ell(\ell+1)}{3(2\ell+1)^3}}\;\left[-2(\ell+1)P_{++} + P_{+-} + 2\ell P_{--}\right] \tag{45}$$

$$\alpha_{12} = +\,\frac{2\mu_n e}{3}\sqrt{\frac{\ell(\ell+1)}{(2\ell+1)^3(2\ell+3)(2\ell-1)}}\;\left[4(\ell+1)(2\ell-1)P_{++}\right.$$

$$\left. - (2\ell-1)(2\ell+3)P_{+-} + 4\ell(2\ell+3)P_{--}\right].$$

We know that $\alpha_{\kappa K} = 0$ for other values of κ and K, and

$$P_{++} = \int \frac{F_+ G_+}{r^2}\,dr$$

$$P_{--} = \int \frac{F_- G_-}{r^2}\,dr \tag{46}$$

$$P_{+-} = \int \frac{F_+ G_- + F_- G_+}{r^2}\,dr\,.$$

For a many-particle configuration, we need make only the substitution $W^{(\kappa K)1} = \sum_{i=1}^{N} w_{(i)}^{(\kappa K)1}$ in (42). We then find that

$$X = \sum_i e_i \alpha \cdot A_i = \alpha_{10} W^{(10)1} + \alpha_{01} W^{(01)1} + \alpha_{12} W^{(12)1} \tag{47}$$

and

$$A = \frac{1}{I}\,\frac{\langle J||X||J\rangle}{\langle J||J||J\rangle}\,. \tag{48}$$

We can further simplify this term by writing

$$W^{(01)1} = \left[\frac{3}{2\ell(\ell+1)(2\ell+1)}\right]^{1/2} \vec{L}$$

$$W^{(10)1} = \left[\frac{2}{(2\ell+1)}\right]^{1/2} \vec{S} \tag{49}$$

$$W^{(12)1} = -\sum_i \left[\frac{(2\ell-1)(2\ell+3)}{\ell(\ell+1)(2\ell+1)}\right]^{1/2} \sqrt{10}\ (\sigma C^2)^1_i \ ,$$

and by using $S = (L + 2S) - J$ and $L = 2J - (L + 2S)$; Equation (47) then becomes

$$X = \alpha\vec{S} + \beta\vec{L} + \gamma \sum_i (\sigma C^2)^1_i \sqrt{10} \ . \tag{50}$$

Using (27) and (50), we then obtain

$$A = \left[(\alpha - \beta + \gamma)(-g_J - 2) + \alpha + \gamma PT(J)\right] \frac{1}{I} \tag{51}$$

where

$$PT(J) = \frac{\left\langle J \| \sum_i N_i \| J \right\rangle}{\left\langle J \| J \| J \right\rangle}$$

$$(\alpha - \beta + \gamma) = + \left[\frac{2}{3}(2\ell-1)(\ell+1)P_{++} - \frac{8}{3}\ell(\ell+1)P_{+-} + \left(\frac{4}{3}\ell^2+2\ell\right)P_{--}\right] \frac{2\mu_n e}{(2\ell+1)^2}$$

$$\alpha = a_{10}\sqrt{2/2\ell+1}$$

$$\gamma = a_{12}\left[\frac{(2\ell-1)(2\ell+3)}{\ell(\ell+1)(2\ell+1)}\right]^{1/2} \ .$$

The term $\frac{\gamma}{I}PT(J)$ is nearly equal to the nonrelativistic A value. Thus the relativistic A value looks very much like the nonrelativistic A value, plus a part depending on g_J and a part constant within a configuration.

In a completely analogous manner we find for the quadrupole moment

$$-\left\langle j \| \frac{1}{r^3} C^2_0 \| j' \right\rangle = \sum_{\kappa K} b_{\kappa K} \left\langle j \| w^{(\kappa K)2} \| j' \right\rangle \tag{52}$$

where

$$b_{11} = -\sqrt{\frac{(4\ell)(\ell+1)}{(25)(2\ell+1)^3}}\ [-(\ell+2)R_{++} + 3R_{+-} + (\ell-1)R_{--}]$$

$$b_{13} = -\sqrt{\frac{6(\ell-1)(\ell)(\ell+1)(\ell+2)}{(25)(2\ell-1)(2\ell+1)^3(2\ell+3)}}\ [(2\ell-1)R_{++} + 4R_{+-} - (2\ell+3)R_{--}] \tag{53}$$

$$b_{02} = \sqrt{\frac{2\ell(\ell+1)}{5(2\ell-1)(2\ell+1)^3(2\ell+3)}}\ [(2\ell-1)(\ell+2)R_{++} + 6R_{+-} + (\ell-1)(2\ell+3)R_{--}].$$

$b_{\kappa K} = 0$ for other κ and K, where

$$R_{++} = \int \frac{F_+^2 + G_+^2}{r^3}\, dr$$

$$R_{--} = \int \frac{F_-^2 + G_-^2}{r^3}\, dr \tag{54}$$

$$R_{+-} = \int \frac{F_+F_- + G_+G_-}{r^3}\, dr.$$

The extension to the many-particle configuration proceeds as above, with

$$Z^2 = -\sum_{i=1}^{N} \frac{1}{r_i^3}\, C^2(i) \tag{55}$$

$$= b_{11}W^{(11)2} + b_{13}W^{(13)2} + b_{02}W^{(02)2}$$

and

$$B = 2e^2Q\ \langle J||Z^2||J\rangle \begin{pmatrix} J & 2 & J \\ -J & 0 & J \end{pmatrix}. \tag{56}$$

In making relativistic calculations, it is useful to have the non-relativistic limits of the radial integrals so that one may at any time pass to the more familiar nonrelativistic equations as a check. As

stated above, in the nonrelativistic limit, ϕ and therefore G goes to zero, and F becomes the nonrelativistic radial wave function R. In addition, F_+ and F_-, as well as G_+ and G_-, approach the same values, because ℓ rather than j becomes more nearly a good quantum number. Thus (41) and (56) can be easily reduced to their nonrelativistic limits. Reduction of the integral $e\int \frac{FG}{r^3}\,dr$, however, is more complicated and requires use of (32).

$$e\int \frac{F_+G_+}{r^2}\,dr \approx \frac{e\hbar}{2mc}\int\left(\frac{F_+}{r^2}\,\frac{dF_+}{dr} - \frac{K}{r}\,F_+\right)dr$$

$$= \frac{e\hbar}{2mc}\int\left(\frac{F_+}{r}\,\frac{d(F_+/r)}{dr} - \frac{\ell}{r}\,F_+^2\right)dr \tag{57}$$

$$= \mu_0\left\{-\ell\,\langle 1/r^3\rangle - \frac{1}{2}\left[(R/r)^2\right]_{r=0}\right\},$$

where in the first step we have set $mc^2 + E + eV_c \approx 2mc^2$. Likewise,

$$e\int \frac{F_-G_-}{r^2}\,dr = \mu_0\left\{(\ell+1)\,\langle 1/r^3\rangle - \frac{1}{2}\left[(R/r)^2\right]_{r=0}\right\} \tag{58a}$$

and

$$e\int \frac{F_+G_- + F_-G_+}{r^2}\,dr = \mu_0\left\{\langle 1/r^3\rangle - \left[(R/r)^2\right]_{r=0}\right\}. \tag{58b}$$

Let us now look at a diagonal element of (40) in the nonrelativistic limit for the case of a single s electron. In this case, $C_1 = 1$, $C_2 = 0$, and $\langle B_J\rangle$ becomes

$$\langle B_J\rangle_z = -\frac{2}{3}\,\mu_0\left[(R/r)^2\right]_{r=0} = -\frac{8\pi}{3}\,\mu_0\,|\psi_0|^2. \tag{59}$$

Then

$$A_s = -\frac{1}{IJ}\,\mu_I B_{Jz} = \frac{16\pi}{3}\,\mu_0^2\,g_I\,|\psi_0|^2$$

as given in (28).

There is another important correction caused by relativistic effects in atomic physics; although it properly belongs in the field of fine structure, it fits most logically into the discussion at this point. This is the "Breit-Margenau"[5] correction to g_J. Calculation of this effect proceeds along the lines of the calculation of the dipole interaction. One introduces a perturbation term $A = -\frac{1}{2} r \times H$, where H is an externally applied field. Then

$$e\sigma \cdot A = -\frac{1}{2} e\sigma \cdot r \times H = -\frac{1}{2} eH \cdot \sigma \times r = +i \frac{\sqrt{2}}{2} eH \cdot (\sigma C^1)^1 r. \tag{60}$$

Comparison with (35) shows that this perturbation term is exactly $(r^3/2)(\vec{H}/\vec{\mu}_I)$ times the operator for the dipole interaction. That is

$$\mathcal{H}^1_{ext} = -\frac{r^3}{2} \frac{\vec{H}}{\vec{\mu}_I} \vec{\mu}_I \cdot \vec{B}_J = -g_J \mu_0 J \cdot H, \tag{61}$$

where the last term on the right is the nonrelativistic operator. We can therefore use the results of (51) with only minor changes. The radial integrals P_{++}, P_{--}, and P_{+-} must be changed to F_{++}, F_{--}, and F_{+-}, where

$$\begin{aligned} F_{++} &= \int r F_+ G_+ dr \\ F_{--} &= \int r F_- G_- dr \\ F_{+-} &= \int r(F_+ G_- + F_- G_+) dr. \end{aligned} \tag{62}$$

These three integrals can be rewritten to make the nonrelativistic limits more obvious. Using (32), we obtain

$$\int r F_\pm G_\pm dr = \frac{\hbar}{2mc} \left(\int 2K_\pm G_\pm^2 \, dr - K_\pm - 1/2 \right)$$

and

$$\int r \, (F_+ G_- + G_+ F_-) dr = -\frac{\hbar}{mc} \int F_+ F_- \, dr. \tag{63}$$

With these forms of the integrals in (51), and multiplying by $(H/2\mu_I)(-1/\mu_0 H)$, we obtain

$$g_J(\text{rel}) = a g_J(\text{nrel}) + b\,PT(J) + c \tag{64}$$

where

$$a = \frac{1}{(2\ell+1)^2}\left[\frac{4}{3}(2\ell^3+3\ell^2-1)\int G_+^2 dr - 4\ell^2\left(\frac{2}{3}\ell+1\right)\int G_-^2 dr + \frac{16}{3}\ell(\ell+1)\int F_+F_- dr - \frac{4}{3}\ell^2 - \frac{4}{3}\ell + 1\right]$$

$$b = a - \int F_+F_- dr$$

$$c = -\frac{2\ell(\ell+1)}{(2\ell+1)^2}\left[(2\ell+2)\int G_+^2 dr - 2\ell\int G_-^2 dr + 2\int F_+F_- dr - 2\right].$$

In the nonrelativistic limit, $G_\pm \to 0$, $F_\pm \to R$, and $a = 1$, $b = c = 0$.

C. Second-Order Effects

The perturbation terms (10) and (14) involving the orbital electrons and the nucleus are not spherically symmetric, and therefore tend to break down both I and J as good quantum numbers. These effects are generally small, and can easily be treated by second-order perturbation theory; they can, however, be very important in cases such as the measurement of anomalies, when very accurate values for A and g_I are required.

Since excited I levels are typically of the order of a few hundred keV above the ground state, and excited J levels of the order of only a few hundred cm^{-1}, we need concern ourselves only with the breakdown of J. The effects of this breakdown can be divided into two groups: effects on terms with energy depending explicitly on the external field (g_I and g_J), and effects on terms not depending explicitly on the field (A, B, etc.).

The values of A, B, etc. are obtained experimentally primarily at low fields, where F is a good quantum number. It is most reasonable, therefore, to look at second-order effects on the interactions (10) and (14) where F is a good quantum number. These effects will have the form

$$\left\langle IJ'FM \middle| Q^{k_1}\cdot F^{k_1} + M^{k_2}\cdot N^{k_2} \middle| IJFM \right\rangle \Big|^2 = (-1)^{2I+2F+2J} \begin{Bmatrix} I & J' & F \\ J & I & k_1 \end{Bmatrix}^2$$

$$\times \left\langle J' \| Q^{k_1} \| J \right\rangle^2 \left\langle I \| F^{k_1} \| I \right\rangle^2$$

$$+ (-1)^{2I+2F+2J} \begin{Bmatrix} I & J' & F \\ J & I & k_2 \end{Bmatrix}^2 \left\langle J' \| M^{k_2} \| J \right\rangle^2 \left\langle I \| N^{k_2} \| I \right\rangle^2$$

$$+ (-1)^{2I+2F+2J}\, 2 \begin{Bmatrix} I & J' & F \\ J & I & k_1 \end{Bmatrix} \begin{Bmatrix} I & J' & F \\ J & I & k_2 \end{Bmatrix}$$

$$\times \left\langle J' \| Q^{k_1} \| J \right\rangle \left\langle J' \| M^{k_2} \| J \right\rangle \left\langle I \| F^{k_1} \| I \right\rangle \left\langle I \| N^{k_2} \| I \right\rangle . \tag{65}$$

We can write the general term

$$(-1)^{F+2I+2J} \begin{Bmatrix} I & J' & F \\ J & I & k_1 \end{Bmatrix} \begin{Bmatrix} I & J' & F \\ J & I & k_2 \end{Bmatrix} = \sum_K C^K \begin{Bmatrix} I & J & F \\ J & I & K \end{Bmatrix} , \tag{66}$$

where

$$C^K = (-1)^{K+k_1+k_2+J'+I} (2K+1) \begin{Bmatrix} k_1 & k_2 & K \\ I & I & I \end{Bmatrix} \begin{Bmatrix} k_1 & k_2 & K \\ J & J & J' \end{Bmatrix} .$$

Insertion of (66) into (65) shows that each of the above second-order perturbation terms looks like a first-order term of rank K, where $k_1 + k_2 \geq K \geq |k_1 - k_2|$. That is, the dipole term can give second-order effects that look like terms from dipoles and quadrupoles.

As values of g_I and g_J are normally obtained from high-field measurements, corrections to these terms will be obtained in the IM_IJM_J system. The term linear in H in the second-order perturbation is of the form

$$\left\langle IM_I JM_J \middle| A^K \cdot B^K \middle| IM_I J' M_J \right\rangle \left\langle IM_I JM_J \middle| \sum \ell_i + 2s_i \middle| IM_I J' M_J \right\rangle H$$

$$= (-1)^{I-M_I} \begin{pmatrix} I & K & I \\ -M_I & 0 & M_I \end{pmatrix} \begin{pmatrix} J & K & J' \\ -M_J & 0 & M_J \end{pmatrix} \begin{pmatrix} J & 1 & J' \\ -M_J & 0 & M_J \end{pmatrix}$$

$$\times \left\langle I \| A^K \| I \right\rangle \left\langle J \| B^K \| J' \right\rangle \left\langle J \| \sum \ell_i + 2s_i \| J' \right\rangle \quad H . \tag{67}$$

Thus, for the transition $\Delta M_I = 0$, $\Delta M_J = \pm 1$, the above term (67), which depends on M_J, will give a contribution to the energy, thereby affecting the measured value of g_J. A like argument shows the above expression will also affect the value of g_I inferred from a $\Delta M_J = 0$, $\Delta M_I = \pm 1$ transition. In particular, the term with $K = 1$ will have an M_I dependence exactly the same as that of $g_I \mu_0 I \cdot H$. Because the M_J dependence, however, can never be the same as that of $g_J \mu_0 J \cdot H$, the possibility exists that by observation of transitions between different pairs of M_J states, an indication of the amount of admixing might be obtained.

D. Exchange Polarization

Many atoms in S states have been shown experimentally to have nonzero values of A, the dipole-interaction constant.[6] The S states, however, are spherically symmetric and should have no hyperfine structure. These nonzero values of A have generally been explained by the mechanism of exchange polarization, which causes contributions to the Fermi contact term from closed shell, or core, electrons.

The approximate Hamiltonian (2) has eigenfunctions of the type of (3), which are products of angular and radial parts. The radial equations obtained from (2) are dependent only on n and ℓ; this dependence results in an R that is equal for all electrons in a shell, regardless of their m_ℓ or m_s dependence. The e^2/r_{ij} perturbation term, however, removes this equivalence through the exchange term $-\left\langle \psi_1(a)\psi_2(b) \middle| e^2/r_{12} \middle| \psi_1(b)\psi_2(a) \right\rangle$. This term is zero for electrons having different m_s, and attractive for electrons of like m_s. Therefore,

because core s electrons having the same value of m_s as the outer valence electrons will be drawn out from the nucleus, a nonzero value of $|\psi_\uparrow(0)|^2 - |\psi_\downarrow(0)|^2$ for two core s electrons in the same shell will result. ($\uparrow$ refers to $m_s = +1/2$, $\downarrow$ to $m_s = -1/2$).

Cohen, Goodings, and Heine[7] used a straightforward application of perturbation methods to calculate the changes in Li and Na of core s functions due to the exchange interaction. They found that when they used bound-state s functions for the terms in the perturbation expansion, the calculated effect was an order of magnitude too small to explain the experimental results. Other calculations[8] have tended to confirm that the bound-state wavefunctions are not a sufficient set of functions for the perturbation problem, but rather that the continuum states must also be considered (therefore providing a complete set).

Although the necessity of including the continuum makes this approach impractical, the perturbation method is valuable in showing the general form of the solution. To second order, the change in A will be given by

$$\Delta A = \frac{32\pi}{3}\frac{\mu_N\mu_0}{I}\sum_{s,s'}\left\langle \ell^N SL, s^2\ {}^1S, SLJ \middle\| \sum s_{zi}\delta(r_i) \middle\| \ell^N S'_1 L'_1, ss'\ {}^{2n+1}S, S'L'J' \right\rangle$$

$$\times \left\langle \ell^N S'_1 L'_1 ss'\ {}^{2n+1}S, S'L'J' \middle| e^2/r_{ij} \middle| \ell^N S_2 L_2, s^2\ {}^1S, S_2 L_2 J_2 \right\rangle$$

$$\times \frac{1}{\langle J \| J \| J\rangle\ (E'_s - E_s)} \quad . \tag{68}$$

The reduced matrix element above is just

$$(-1)^{L+J'+S'}\ \frac{2}{\sqrt{2}}\ \begin{Bmatrix} J & 1 & J' \\ S' & L & S \end{Bmatrix} \left(\frac{[J][J'][S']}{[1/2][1]}\right)^{1/2} \langle s \| s\delta(r) \| s'\rangle$$

$$\times\ \delta(L, L')\delta(S, S')\delta(n, 1).$$

From this we see that only the triplet state of ss' is important in second order.

The matrix element of e^2/r_{ij} with n = 1 can easily be obtained from the work of Rajnak and Wybourne[9]; it is

$$(-1)^{S_2-S_1'} \frac{[1/2]^{1/2}}{[S_2]} \langle S||S||S'\rangle R^{\ell}(\ell s', s\ell)\delta(J', J_2)\delta(S', S_2)\delta(L', L_2)\delta(L_2, L_1').$$

Combining these two expressions gives

$$\langle SLJ||S||SLJ'\rangle \frac{\psi_s(0)\psi_{s'}(0)}{[\ell]} R^{\ell}(\ell s', s\ell)\delta(L, L')\delta(S'S)\delta(n, 1)\delta(n, 1)$$

$$\times \quad \delta(J', J_2)\delta(S', S_2)\delta(L', L_\delta)\delta(L_2 L'_1).$$

If $J = J'$, we can write $S = L + 2S - J$, and $\frac{\langle J||S||J\rangle}{\langle J||J||J\rangle} = -g_J - 1$,

making

$$\Delta A = -(g_J + 1) \frac{32\pi}{3} \frac{\mu_N \mu_0}{I} \sum_{ss'} \frac{R^{\ell}(\ell s', s\ell)}{[\ell]} \frac{\psi_s(0)\psi_{s'}(0)}{\Delta ss'} \tag{69}$$

for all levels of the configuration ℓ^N. Higher order terms will not have this same dependence on L, S, and J, but should be much smaller. Then

$$A = A_1 + \Delta A + B, \tag{70}$$

where A_1 is given by (25), ΔA by (69), and B includes the higher order terms. If B is negligibly small, we see that (70) has the same J dependence as (51). This means that one cannot easily separate contributions to A from core polarization and relativity.

An alternative approach to the problem of exchange polarization is offered by the spin-polarized Hartree-Fock method. In this method, one solves two Hartree-Fock equations per shell, one for each m_s projection. These equations will have slightly different potentials

because of the exchange term with the valence electron.

This method should make it possible to predict all effects of promoting core s electrons to higher s states, but does not include the effect of promoting s electrons to d states; this is a third-order effect and should usually be small, however.

E. Hyperfine Anomalies

According to (25), the A values of two isotopes of the same element should be related by

$$\frac{A_1}{A_2} = \frac{\mu_I(1)B_J(1)I_2}{\mu_I(2)B_J(2)I_1} = \frac{g_I(1)}{g_I(2)} \quad . \tag{71}$$

Here $B_J(1) = B_J(2)$, because B_J is a function of the electronic rather than the nuclear properties of the atom. Deviations from (71) occur, however, and these deviations are expressed in terms of an anomaly ${}_i\Delta_j$,

$$(1 + {}_1\Delta_2)\ \frac{g_I(1)}{g_I(2)} = \frac{A_1}{A_2} \quad . \tag{72}$$

In the heavier elements, Δ arises from errors associated with the assumption that μ_I is a point dipole. The two largest corrections, the Bohr-Weisskopf[10] and Breit-Rosenthal[11] corrections, arise from finite-volume distributions of the nuclear magnetization and of the nuclear charge, respectively.

In the Bohr-Weisskopf correction, we assume that the nucleus has a magnetic-dipole density $\omega(R)$ associated with the nuclear spin $\vec{S}$ this density gives rise to an A_S at the electron position $\vec{r}$ of

$$A_S(r) = -\int d\tau_n\, \omega(R) g_s S(n) \times \nabla_r \frac{1}{|\vec{r} - \vec{R}|} \quad ,$$

where g_s is the g factor of the spin. We can write the contribution to A from the orbital momentum A_L as

$$A_L(r) = \frac{1}{c}\int \frac{j}{|r - R|}\, d\tau_n = \frac{ze}{m_n c}\int \psi_n^* \frac{\vec{P}}{|r - R|}\, \psi_n\, d\tau_n \, .$$

We must then substitute the sum $A = A_L + A_S$ for A as given in (34) into (33).

Electrons $S_{1/2}$ and $P_{1/2}$ are the only ones with nonzero densities near the nucleus; they are therefore the only ones that will be affected by the finite nuclear size. For $S_{1/2}$ and $P_{1/2}$ electrons, we can make the simplification

$$e\int \psi^* \alpha \cdot A\psi d\tau_e = \pm \frac{2e}{4\pi} \int d\tau_e \frac{FG}{r^3} (\vec{A} \times \vec{r})_z ,$$

where +(-) refers to the $S_{1/2}(P_{1/2})$ state. This simplification is done by expanding the angular parts of ψ into sums of $\ell m_\ell s m_s$ wave-functions, operating with $\sigma \cdot A = \sigma_z A_z + \sigma_+ A_- + \sigma_- A_+$, and integrating over the spin coordinates. Then for the energy due to the spin moment, we write

$$W_S = \pm \frac{2e}{4\pi} e\int d\tau_e \frac{FG}{r^3} \left[\vec{r} \times \int d\tau_n g_s \omega(R) (\vec{S}(n) \times \vec{\nabla}_r \frac{1}{|r-R|} \right]_z$$

$$= \pm \frac{2e}{4\pi} \int d\tau_n \omega(R) g_s \int d\tau_e \frac{FG}{r^2} \left\{ S_z(n) \left(\frac{\vec{r}}{r} \cdot \vec{\nabla}_r \frac{1}{|r-R|} \right) - \left(\nabla_r \frac{1}{|r-R|} \right)_z \right.$$

$$\left. \times \left[\frac{\vec{r}}{r} \cdot \vec{S}(n) \right] \right\} .$$

Because $S_{1/2}$ and $P_{1/2}$ electrons have nonzero density at the origin, and thereby penetrate into the nucleus, we must make expansions of $\frac{1}{|r-R|}$ for both $r > R$ and $r < R$. The problem is simplified because the nature of the integral over the electron coordinates shows that the only expansion term that can have a nonzero effect is that containing $Y_0^0(\theta_e \phi_e)$. Performing the indicated operations yields

$$W_S = \pm \frac{4}{3} \int d\tau_n \omega(R) g_s S_z(n) \left[\int_R^\infty \frac{FG}{r^2} dr - \zeta \int_0^R \frac{r}{R^3} FG\, dr \right] , \tag{73}$$

where

$$\zeta = \frac{1}{S_z} \left[\vec{\sigma} - \frac{3(\sigma \cdot R)\vec{R}}{R^2} \right]_z .$$

The energy due to a point dipole would be

$$W_S^0 = \frac{4e}{3} \int d\tau_n \omega(R) g_s S_z \int_0^\infty \frac{FG}{r^2} \, dr. \tag{74}$$

We can therefore write

$$W_S = W_S^0 (1 - K_S), \tag{75}$$

where

$$K_S = \frac{\int_0^R \left(\frac{1}{r^2} + \zeta \frac{r}{R^3}\right) FG \, dr}{\int_0^\infty \frac{FG}{r^2} \, dr} .$$

In a like manner we obtain

$$W_L = \frac{4e}{3} \int d\tau_n \omega(R) g_L L_z \left[\int_R^\infty \frac{FG}{r^2} \, dr + \int_0^R \frac{r}{R^3} \, FG \, dr \right]. \tag{76}$$

The energy in the point-dipole approximation is

$$W_L^0 = \frac{4e}{3} \int d\tau_n \omega(R) g_L L_z \int_0^\infty \frac{FG}{r^2} \, dr, \tag{77}$$

leading to

$$W_L = W_L^0 (1 - K_L), \tag{78}$$

where

$$K_L = \frac{\int_0^R \left(\frac{r}{R^3} + \frac{1}{r^2}\right) FG \, dr}{\int_0^\infty \frac{FG}{r^2} \, dr} .$$

If α_S is the fraction of total-hyperfine-structure energy due to the spin moment, and α_L is that due to the orbital moment, then

$$W = W_0(1 - \alpha_S K_S - \alpha_L K_L)$$
$$= W_0(1 - \epsilon). \tag{79}$$

The effect of finite volume of nuclear charge is to change the values of F and G within the nucleus from the values of F_0 and G_0 obtained for a point nucleus. This correction can be incorporated into the above corrections by writing

$$K_S = \frac{\int_0^R \left(\frac{1}{r^2} + \zeta \frac{r}{R^3}\right) FG\, dr}{\int_0^\infty \frac{F_0 G_0}{r^2}\, dr}$$

and (80)

$$K_L = \frac{\int_0^R \left(\frac{1}{r^2} + \frac{r}{R^3}\right) FG\, dr}{\int_0^\infty \frac{F_0 G_0}{r^2}\, dr} ,$$

where F, G are the true radial functions within the nucleus.

Then

$$\frac{g_I(1)}{g_I(2)} \frac{(1 - \epsilon_1)}{(1 - \epsilon_2)} = \frac{W_1}{W_2} = \frac{A_1}{A_2} , \tag{81}$$

and from (72), we see that

$${}_1\Delta_2 = \frac{\epsilon_2 - \epsilon_1}{1 - \epsilon_2} . \tag{82}$$

F. Collective Model of the Nucleus

In this model a long-range correlation between the nucleons causes a relatively long term stability in the nuclear shape; that is, the particles move in some collective motion. We may view such correlation as being a result of coupling between particle and nuclear

surface. The particle moves in a nonspherically symmetric field caused by a distortion of the nuclear surface; because of its motion, the particle itself will then provide a nonspherically symmetric potential in which the other particles move.

The simplest deformed body to consider is the ellipsoid, with

$$R = R_0 \left[1 + \sum_m a_m Y_m^2(\theta', \phi') \right], \tag{83a}$$

where θ', ϕ' are angles with respect to the principle axes of the nucleus. The constants a_m can be written

$$\begin{aligned} a_0 &= \beta \cos \gamma \\ a_{\pm 2} &= \frac{1}{\sqrt{2}} \beta \sin \gamma \\ a_{\pm 1} &= 0 . \end{aligned} \tag{83b}$$

In the laboratory system, the Hamiltonian of the ellipsoid exclusive of center-of-mass motion can be written

$$\mathcal{H} = \frac{1}{2} \sum_m B |\dot{\alpha}_m|^2 + \frac{1}{2} \sum_m C |\alpha_m|^2 \tag{84}$$

if we assume a harmonic-oscillator-type potential.

The α_m's are the deformation parameters corresponding to the a_m's obtained when R is expressed in terms of space-fixed axes.

Manipulation of (84) then gives

$$\mathcal{H} = \mathcal{H}(\beta\gamma) + \mathcal{H}_{rot} , \tag{85}$$

where

$$\mathcal{H}_{rot} = \sum_{K=1}^{3} \frac{L_K^2}{2\mathfrak{J}_K} \tag{86}$$

with $\mathfrak{J}_K = 4B\beta^2 \sin^2(\gamma - K \frac{2\pi}{3})$. If $\mathfrak{J}_1 = \mathfrak{J}_2 = \mathfrak{J}$, $\mathcal{H}_{rot}$ is the Hamiltonian for the symmetric top, with eigenfunctions of the type $D^R_{\alpha\delta}(\Theta\ \Phi\ \Psi)$. The rotational constants of the collective nucleus are

therefore $L^2 = R(R+1)$, $L_z = \alpha$ (z is the space-fixed axis), and $L_3 = \delta$ (3 is the body-symmetry axis).

Let us now assume there are one or two unpaired particles of total angular momentum $\vec{j}$ outside the core. The total Hamiltonian will then become

$$\mathcal{H} = \mathcal{H}(\beta\gamma) + \mathcal{H}_{rot} + \mathcal{H}_p$$

where $\mathcal{H}_p$ is the single-particle Hamiltonian.

The angular momentum of the last particles will couple to that of the core to give a total angular momentum: $\vec{j} + \vec{R} = \vec{I}$. Let us express (86) in terms of I:

$$\mathcal{H}_{rot} = \sum_{K=1}^{3} \frac{R_K^2}{2\mathfrak{J}_K} = \sum_{K=1}^{3} \frac{(I_K - j_K)^2}{2\mathfrak{J}_K} = \frac{\hbar^2}{2\mathfrak{J}} \left[(I-j)^2 - (I_3 - j_3)^2 \right] + \frac{\hbar^2}{2\mathfrak{J}_3} (I_3 - j_3)^2.$$

Because of the axial symmetry of the core potential, $\mathcal{H}_p$ will be diagonal in $j_3 = \Omega$. The total Hamiltonian will be diagonal with respect to $I_z = M$, but not necessarily with respect to $I_3 = K$. When these quantum numbers are used, (86) becomes

$$\mathcal{H}_{rot} = \frac{\hbar^2}{2\mathfrak{J}} \left[I(I+1) - K^2 - \Omega^2 \right] + \frac{\hbar^2}{2\mathfrak{J}_3} (K - \Omega)^2 - \frac{\hbar^2}{2\mathfrak{J}} (I_+ j_- + I_- j_+) + \frac{\hbar^2}{2\mathfrak{J}} \vec{j}^2. \tag{87}$$

For low-lying states, $\mathfrak{J}_3$ is very small, and $\mathcal{H}_{rot}$ will be minimum for $K = \Omega$. The term $I_+ j_-$ tends to break down K as a good quantum number, but when $K = \Omega$, a perturbation calculation shows this breakdown is negligible. That is, states of different K correspond to different single-particle states, and the very large difference in single-particle energies in the denominator of the perturbation coefficient makes the coefficient go to zero. Since neither $\mathcal{H}(\beta\gamma)$ nor $\mathcal{H}_p$ depend on K, $K = \Omega$ will also be a minimum for $\mathcal{H}$.

Let us define

$$\left(\mathcal{H}_p + \frac{\hbar^2}{2\mathfrak{J}} \vec{j}^2 \right) \chi_\Omega = \mathcal{H}_0 \chi_\Omega = \epsilon_\Omega \chi_\Omega. \tag{88}$$

Then an eigenfunction of (87) (neglecting the term in $j_+ I_-$) invariant under rotations around the symmetry axis is

$$\Psi(IMK\Omega) = \left(\frac{2I+1}{16\pi^2}\right)^{1/2} \left[D^I_{MK}\chi_\Omega + (-1)^{I+K+\Omega} D^I_{M-K} \sum_j (-1)^j C_{j\Omega}\chi_{j\Omega}\right], \tag{89}$$

where we write $\chi_\Omega = \sum_j C_{j\Omega}\chi_{j\Omega}$ because j_3 and not j^2 is a good quantum number.

We now take a diagonal element of (87), using (89) and letting $K = \Omega$.

$$E_{IK} = \epsilon_K + \frac{\hbar^2}{2\mathfrak{J}} \left[I(I+1) - 2K^2 + \delta_{K\frac{1}{2}}\, \delta_{\Omega\frac{1}{2}} (-1)^{I+\frac{1}{2}} (I+\tfrac{1}{2})a\right] . \tag{90}$$

Here a is the decoupling parameter

$a = -\sum_j (-1)^{j+\frac{1}{2}}(j+\frac{1}{2})\left|C_{j\frac{1}{2}}\right|^2$. The last term on the right (90) is the only nonzero diagonal term arising from the I_+j_- term in (87). [In obtaining (90), one must remember that I_3 refers to the component of a space-fixed vector along a moving axis, and $(I_1, I_2) = -iI_3$, etc.] We see from (90) that when $K \neq \frac{1}{2}$, the minimum value of E_{IK} occurs for $I = +|K|$.

We can now consider the term ϵ_K. One must make some sort of assumption concerning the nature of the potential between the unpaired nucleons and the core. Nilsson[12] has assumed an isotropic harmonic oscillator potential, with a $C\ell\cdot s$ term added to provide agreement with the shell model near closed shells, and a $D\ell^2$ term to make the potential more like a square well for large values of ℓ. The harmonic oscillator has $\omega_1^2 = \omega_2^2 = (1 + \frac{2}{3}\delta)\omega_0^2$, $\omega_3^2 = (1 - \frac{4}{3}\delta)\omega_0^2$, with $\delta = \sqrt{\frac{45}{16\pi}}\,\beta \approx \beta$. Then $\mathcal{H}_p$ mixes in states with $\ell' = \ell \pm 2$, and breaks down Λ and Σ, the three projections of the particle's angular momentum ℓ and spin s. For very large deformations, Λ and n_3 (the harmonic-oscillator quantum numbers along the 3 axis) become good quantum numbers. Nilsson therefore labels his states by their large deformation quantum numbers $|Nn_3\Lambda\Omega\rangle$. At intermediate deformations this can be expressed as

$$\left|Nn_3\Lambda\Omega\right\rangle = \sum_{\ell n\Sigma} a_{\ell n\Sigma}\left|N\ell\Lambda\Sigma\right\rangle. \tag{91}$$

This type of Hamiltonian gives equal energies for states of both $+\Omega$ and $-\Omega$. This equality causes problems in the determination of ground state I's when there are two unpaired nucleons outside the core. That is, the states with $\Omega_a = \Omega_1 + \Omega_2$ and $\Omega_b = |\Omega_1 - \Omega_2|$ are degenerate, and K and therefore I can equal either. Gallagher and Moszkowski[13] have predicted that the spins of the two odd particles tend to align themselves parallel to each other, so that $\Omega = \Omega_1 + \Omega_2$ if $\Omega_1 = \Lambda_1 \pm \frac{1}{2}$, $\Omega_2 = \Lambda_2 \pm \frac{1}{2}$; $\Omega = |\Omega_1 - \Omega_2|$ if $\Omega_1 = \Lambda_1 \pm \frac{1}{2}$, $\Omega_2 = \Lambda_1 \mp \frac{1}{2}$.

Using the above relations, we can now calculate the nuclear dipole and quadrupole moments. The magnetic dipole moment is given by

$$\mu_I = \left\langle g_s s_z + g_\ell \ell_z + g_R R_z \right\rangle_{M_I = I} = \frac{1}{I+1}\left[(g_R)\left\langle I\cdot I\right\rangle + (g_s - g_\ell)\left\langle S\cdot I\right\rangle + (g_\ell - g_R)\left\langle j\cdot I\right\rangle\right]$$

$$= \frac{I}{I+1}\left[g_\ell I + g_R + \frac{1}{2}(g_s - g_\ell)\sum_\ell (a^2_{\ell\uparrow} - a^2_{\ell\downarrow})\right] \tag{92}$$

for a single unpaired particle, and

$$\mu_I = \frac{I}{I+1}\left[g_R + g_{\ell p}\Omega_p + \frac{1}{2}(g_{sp} - g_{\ell p})\sum_{\ell p}(a^2_{\ell\uparrow} - a^2_{\ell\downarrow})\right.$$

$$\left. \pm \frac{1}{2} g_{sn}\sum_{\ell n}(a^2_{\ell\uparrow} - a^2_{\ell\downarrow})\right] \tag{93}$$

for two unpaired particles.

In (91), one uses $\pm$ for $\Omega = \Omega_p \pm \Omega_n$. If $\Omega = \Omega_n - \Omega_p$, then the signs of the second and third terms must be made negative. Equations (90) and (91) hold only if $K \neq 1/2$.

The total quadrupole moment is the sum of the single-particle and core moments. In the range of validity of the Nilsson model, the former is much smaller than the latter and can be neglected. We define Q_s as the core quadrupole moment as measured in the

laboratory system, and Q_0 as the moment with respect to the nuclear axes. Then

$$Q_s = \sqrt{\frac{8\pi}{5}} \left\langle IMK \middle| \sum_{n=1}^{A} q_n Y_0^2 (\theta_n \phi_n) r_n^2 \middle| IMK \right\rangle$$

$$= \sqrt{\frac{8\pi}{5}} \left\langle IMK \middle| \sum_n \sum_m q_n Y_m^2 (\theta_n' \phi_n') D_{0M}^2 (\Theta \Phi \Psi) \middle| IMK \right\rangle$$

$$= \sqrt{\frac{8\pi}{5}} \left\langle IMK \middle| D_{00}^2 \middle| IMK \right\rangle \left\langle IMK \middle| \sum_n q_n Y_0^2 (\theta_n' \phi_n') r_n^2 \middle| IMK \right\rangle$$

$$= \frac{3K^2 - I(I+1)}{(I+1)(2I+3)} Q_0 . \tag{94}$$

We see from (83) that for the 3 axis to be a symmetry axis, $\gamma = 0°$, and $R = R_0 [1 + \beta Y_0^2 (\theta\phi)]$. Then if we assume $\rho(r)$ equal to a constant, and $\int \rho(r) dv$ equal to Z,

$$Q_0 = \int r^2 (3 \cos^2\theta - 1) \rho(r) dv$$

$$= \sqrt{\frac{16\pi}{5}} \int Y_0^2 (\theta\phi) d\psi_0 \int_0^{R_0(1+\beta Y_0^2)} \rho(r) r^4 dr \tag{95}$$

$$\cong 0.8 \, Z R_0^2 \beta$$

to first order in β.

III. EXPERIMENTAL METHOD

The atomic-beam method utilizes two regions of a large and inhomogeneous magnetic field and one of a constant magnetic field to measure atomic-energy differences arising from the hyperfine interactions. A beam machine of the "flop-in" design is shown in Fig 1; in this machine the two regions of inhomogeneous field (produced by the A and B magnets) have their gradients in the same direction. In these two regions, the atoms "feel" a force given by $F_Z = -\frac{\partial \mathcal{H}_{ext}}{\partial Z} \approx g_J \mu_0 M_J \frac{\partial H}{\partial Z}$. This latter equation is obtained by evaluating $\mathcal{H}_{ext}$ as defined above (17) in the Paschen-Back region and neglecting the term in g_I, which is about 1/2000 of g_J. In order to be detected, an atom must have its deflection in the A region cancelled by its deflection in the B region; this cancellation can occur if $M_J(A) = -M_J(B)$. This condition requires that the atom undergo a transition in the C region. Transitions are induced by introducing into the C region a small magnetic field oscillating at the Bohr frequency of the atom in the constant (and large relative to the oscillating field) C field.

Exact transition probabilities, in general difficult to calculate, depend on such things as the relative strengths of the static and oscillating fields, the velocity spectrum of the beam, and the number of possible transitions occurring at frequencies near the Bohr frequency of the desired transition. Two common results should be noted, however. First is that (single quantum) transitions occur when the oscillating frequency is equal to the Bohr frequency of the atom, i.e., $\nu = \frac{E_1 - E_2}{h}$. Second is that the probability will depend in some way on $|\langle \psi_f | \mathcal{H}_{pert} | \psi_i \rangle|^2$, where, in this case, $\mathcal{H}_{pert} = -g_J \mu_0 J \cdot H' - g_I \mu_0 I \cdot H'$. Depending on the type of transition to be induced, H' is either $H_0 \cos \omega t \hat{i} + H_0 \sin \omega t \hat{j}$ or $H_0 \cos \omega t \hat{k}$. In the first case $\mathcal{H}_{pert}$ can be written (neglecting the term in g_I) as $\frac{\mu_0 H_0}{2} (J_- e^{i\omega t} + J_+ e^{-i\omega t})$; in the second as $\frac{\mu_0 H_0}{2} J_Z (e^{i\omega t} + e^{-i\omega t})$. The first term obviously connects states differing by ± 1 in m_J,

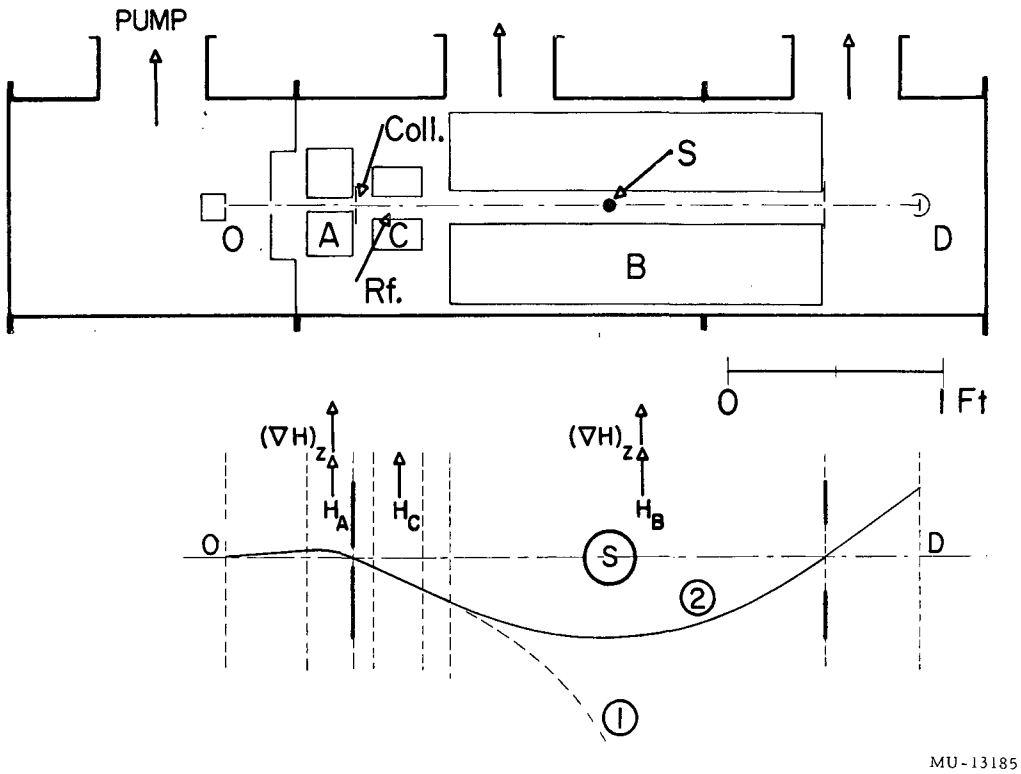

Fig. 1. Schematic arrangement and trajectory in an atomic-beam flop-in apparatus.

and the second is diagonal in m_J. Simple conservation-of-energy and -momentum considerations show that left-handed polarized photons ($m_\ell = 1$) will cause $\Delta M = \pm 1$ transitions if $E_m > E_{m-1}$, and right-handed polarized photons ($m_\ell = -1$) will do the same if $E_m < E_{m-1}$.

If $|\langle \psi_f | \mathcal{H}_{pert} | \psi_i \rangle|^2$ is taken in the low-field representation, the allowed transitions are $\Delta M_F = 0, \pm 1$, and $\Delta F = 0, \pm 1$. If it is taken in the high-field representation, the allowed transitions are $\Delta M_J = 0, \pm 1$; $\Delta M_I = \pm 1, 0$; or $\Delta M_J = \Delta M_I = 0$.

The limitations on observable transitions by the beam machine $[M_J(A) = -M_J(B)]$ and by the transition probabilities for magnetic-dipole transitions means that only transitions labeled by Greek letters in Figs. 6, 7, and 8 can ordinarily be observed in a beam machine. These transitions can be described as one of two types: (a) $\Delta F = 0$, $\Delta M_F = \pm 1$ in low field, and $\Delta M_J = \pm 1$, $\Delta M_I = 0$ in high field; or (b) $\Delta F = \pm 1$, $\Delta M_F = 0$ in low field, and forbidden in high field. The former has a low-field field-dependent part $\mu_0 H[\frac{F(F+1)+J(J+1)-I(I+1)}{2F(F+1)} g_J + \frac{F(F+1)+I(I+1)-J(J+1)}{2F(F+1)} g_I]$, and a high-field field-dependent part $\mu_0 H g_J$. Because g_I is about 1/2000 of g_J, the low-field dependence on g_I of this transition is almost undetectable in most beam machines. The latter transition is used to fix the constants A, B, and C because of its independence (to first order) of g_I, g_J, and H. These two types of transitions are therefore relatively insensitive to g_I.

The triple-resonance method[14] allows one to observe transitions that are in the high-field limit $\Delta M_I = \pm 1$, $\Delta M_J = 0$. These transitions are labeled by numbers in Figs. 6, 7, and 8. The field-dependent part of this transition is just $g_I \mu_0 H$, which allows precise measurement of the value of g_I. This method consists of subjecting the atoms to the frequencies of, first, an ordinary resonance of the first type described above, then one of the $\Delta M_I = \pm 1$, $\Delta M_J = 0$ resonances, and finally to the first frequency again. The energy levels involved are shown schematically in Fig. 2.

One can then calculate the signal strength for one, two, and three hairpins. If the probability of inducing a transition in the A hairpin is P_A, then

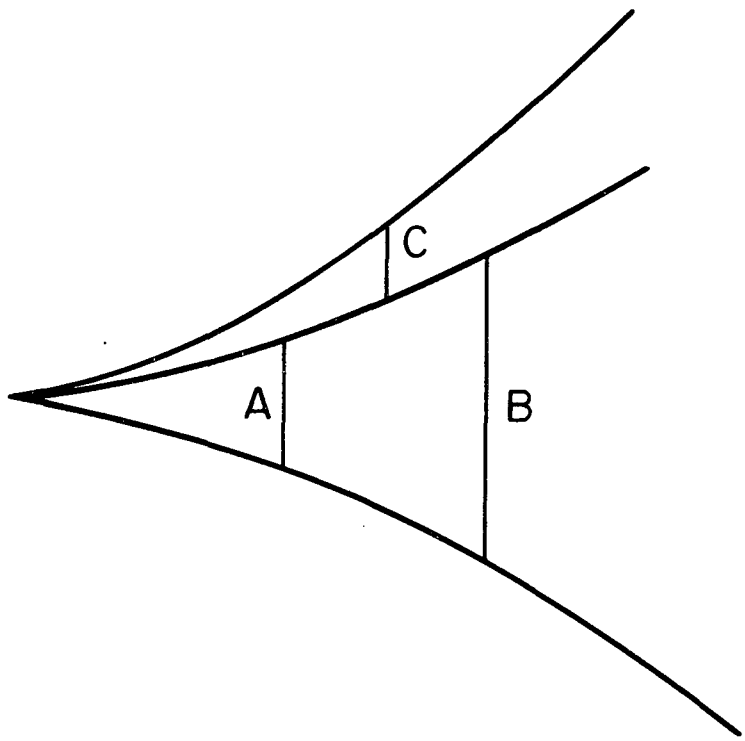

MUB-8117

Fig. 2. Triple-loop signal equations:

$$S_A = 2n\,P_A$$
$$S_{AB} = 2n\,(P_A + P_B - 2P_AP_B)$$
$$S_{ABC} = 2n\,(P_A + P_B - 2P_AP_B + P_AP_BP_C)$$

$$S_A = 2nP_A,$$

where we have assumed all hyperfine levels to be equally populated with n particles. Likewise

$$S_{AB} = 2nP_A(1 - P_B) + 2n(1 - P_A)P_B$$
$$= 2n(P_A + P_B - 2P_AP_B)$$

and

$$S_{ABC} = 2n(P_A + P_B - 2P_AP_B + P_AP_BP_C).$$

Thus if P_A and P_B are nonzero and constant, the signal strength will vary as P_C. This relationship enables one to trace out a resonance with $\Delta M_I = \pm 1$, $\Delta M_J = 0$, thus allowing g_I to be measured directly.

IV. APPARATUS

The machine used for both experiments was essentially that described by White.[15] Consequently the only details discussed here are those in which the machine differs from this earlier description.

The most important difference was the positioning of three hairpins, rather than just one, in the C-magnet region (Fig. 3). The individual hairpins were 3/4-in. long in the beam direction and roughly 1 in. apart. The two end hairpins, being nearer to the A and B magnets, respectively, were in much less homogeneous fields than was the center hairpin. Resonance line widths at high fields in the end hairpins were therefore 3 to 6 times as broad as those in the center hairpin.

During these experiments the A and B magnets were driven in series by the B-magnet supply. The A-magnet supply, which had better regulation than the C-magnet supply, was modified to drive the C magnet. Although the resulting C-magnet power supply could drive the C magnet to only slightly above 700 G rather than to 1000 G, as had the previous supply, regulation was much improved.

The early work on Re was done with an oven loader like that described by Schlecht,[16] and the later Re work and all of the Am work was done with the oven loader shown in Fig. 4. Because this latter oven loader allowed the sample to be placed nearer the entrance to the A magnet than had the previous loader, signal intensities were increased. The radio-frequency equipment used is listed in Table I.

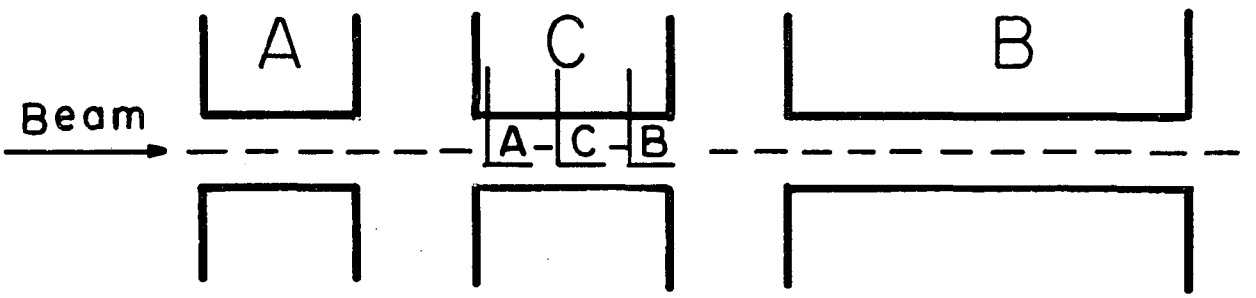

MUB-4246

Fig. 3. Schematic of magnets and hairpins.

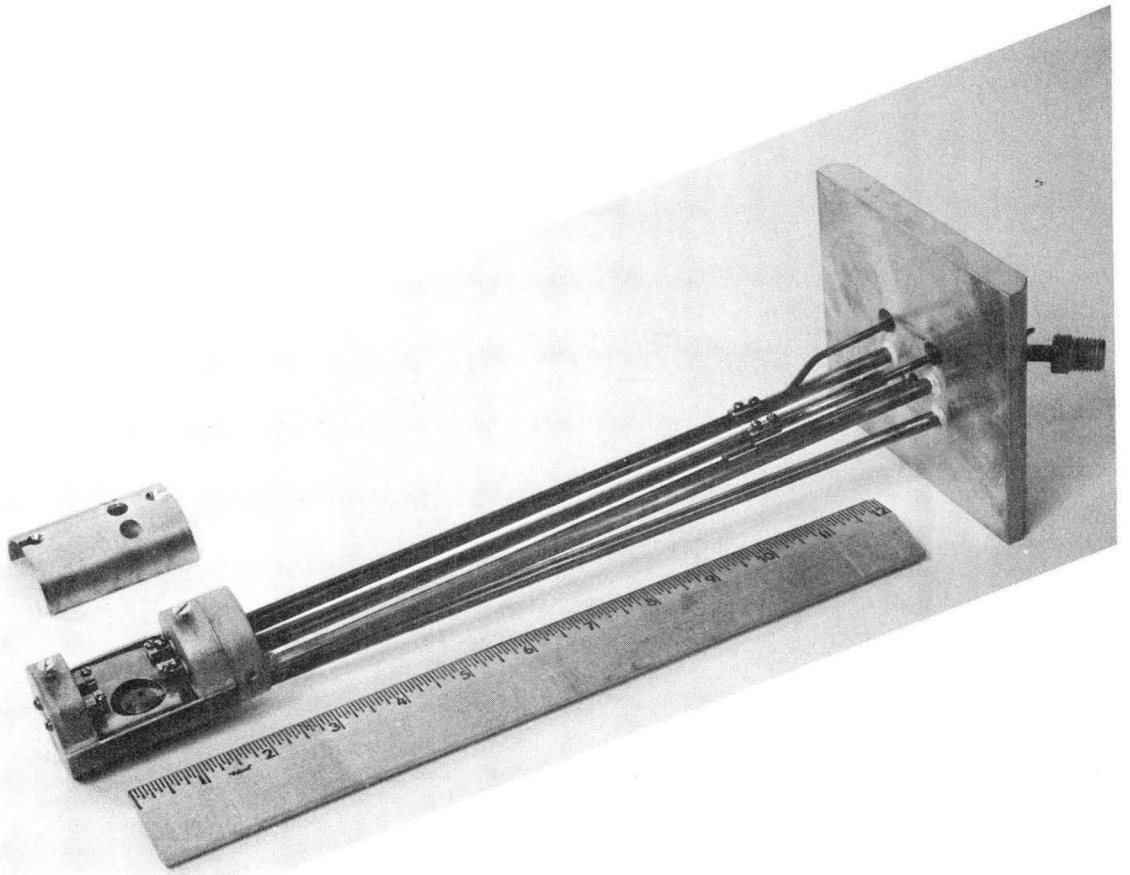

ZN-5189

Fig. 4. Oven loader used for Re and Am.

Table I. Radio-frequency equipment.

Instrument	Frequency range (Mc/sec)
Oscillators:	
Hewlett-Packard 608C	10.0 to 480.0
Tektronix 190A	0.35 to 50.0
General Radio 1208B	65.0 to 500.0
General Radio 1209B	250.0 to 920.0
General Radio 1218A	900.0 to 2000.0
Rohde and Schwarz SLRD	275.0 to 2750.0
Hewlett-Packard 540A transfer oscillator	100.0 to 220.0
Amplifiers:	
IFI 500 wide-band amplifier	0.5 to 240.0
IFI 510 wide-band amplifier	0.5 to 240.0
Frequency-measuring instruments:	
Hewlett-Packard 524B electronic counter	0.0 to 10.0
Hewlett-Packard 5245L electronic counter	0.0 to 100.0
Hewlett-Packard 525A frequency converter	0.0 to 100.0
Hewlett-Packard 525B frequency converter	100.0 to 220.0
Hewlett-Packard 525C frequency converter	100.0 to 500.0
Hewlett-Packard 5253B frequency converter	50.0 to 500.0
Hewlett-Packard 5254A frequency converter	300.0 to 3000.0
Northeastern Engineering 14-26C frequency converter	200.0 to 1000.0

V. RHENIUM

A. Introduction

The research on rhenium was undertaken primarily for two reasons. First, the ground configuration of Re is a half-filled shell in the Hund's rule ground state, which in this case is $(5d)^5(6s)^2\ {}^6S_{5/2}$. The spherical symmetry of such states indicates that at the nucleus there are no hyperfine fields caused by the electrons in the half-filled shell; other effects such as core polarization and relativity then become dominant and are more easily studied. Second, Re is in a state of intermediate deformation according to the Nilsson nuclear model, and it is of interest to see if the model is still valid in this region.

The starting point is the work of Schlecht, White, and McColm,[17] who measured to high precision g_J and the hyperfine constants A and B for both Re^{186} and Re^{188}. The interpretation of our results was greatly aided by Trees'[18] analysis of the optical spectrum of Re, which included the effects of both breakdown of LS coupling and configuration mixing.

B. Experimental Method and Results

Beams of Re were obtained by electron bombardment of 20-mil Re wires. In this method, the Re wire is placed near a W wire that has sufficient current passing through it to produce large emission currents. The Re wire is then made to act as a collector by being biased to a positive voltage. The Re wires were of natural Re that had been bombarded at a flux of 10^{14} neutrons/cm-sec for either 4 hours (to produce Re^{188}) or 3 days (to produce Re^{186}). A detailed description of the irradiation procedures and the oven loaders used for electron bombardment of wires is given by Schlecht.[16]

As indicated in Sec. III, in our experiment the A and B hairpins were set on the $\Delta F = 0$, $\Delta M_F = \pm 1$ transition and the signal from each hairpin was maximized separately. This then led to a minimum signal for A and B together. In practice a signal-to-noise ratio of about 10:1 could be obtained in each hairpin separately, and the two-hairpin signal was only slightly above background. This low level indicated that both P_A and P_B were near unity. The C-hairpin frequency was then varied, and signal-to-noise ratios of about 8:1 or 9:1 could

be obtained with the triple-loop resonance. At the C fields used (200 to 500 G), the line widths in the A and B hairpins were 300 to 400 kc/sec. This meant that the C field could drift about 60 kc/sec without significantly affecting either P_A or P_B. Triple-resonance lines at these fields were approximately 25 kc/sec wide. Some observed triple-resonance lines are shown in Fig. 5.

Figure 6 is a schematic of the hyperfine levels of both Re isotopes. The A and B hairpins were set on the resonance β, (5/2, +1/2) ⟷ (5/2, -1/2). The triple resonances observed are numbered 1, 3, and 4. Resonance number 2 was not observed, probably because the right power was not used in the C hairpin. The C-hairpin resonances were very power sensitive, and the power required for us to observe the different transitions at one field setting varied considerably, sometimes by a factor of 100.

The data obtained by the triple-resonance method were combined with that of Schlecht et al.[12] for purposes of data reduction. The combined observations were fitted to a Hamiltonian of the form

$$\mathcal{H} = AI\cdot J + \frac{B[3(I\cdot J)^2 + 3/2(I\cdot J) - I(I+1)J(J+1)]}{2IJ(2I-1)(2J-1)} - g_J\mu_0 J\cdot H - g_I\mu_0 I\cdot H \tag{96}$$

by means of the IBM 7090 program HYPERFINE 4. Values of A, B, g_J, and g_I were all varied. The final results are (Table II):

<u>Re^{186}</u>

$A = \pm\ 78.3060(10)$ Mc/sec
$B = \mp\ 8.3595(16)$ Mc/sec
$g_J = -\ 1.951988(39)$
$g_I = +\ 9.34(2) \times 10^{-4}$

<u>Re^{188}</u>

$A = \pm\ 80.4326(8)$ Mc/sec
$B = \mp\ 7.7463(11)$ Mc/sec
$g_J = -\ 1.952072(60)$
$g_I = +\ 9.61(3) \times 10^{-4}$

The values of g_J, A, and B are essentially those of Schlecht et al.[17] The triple resonances fix the value of g_I only.

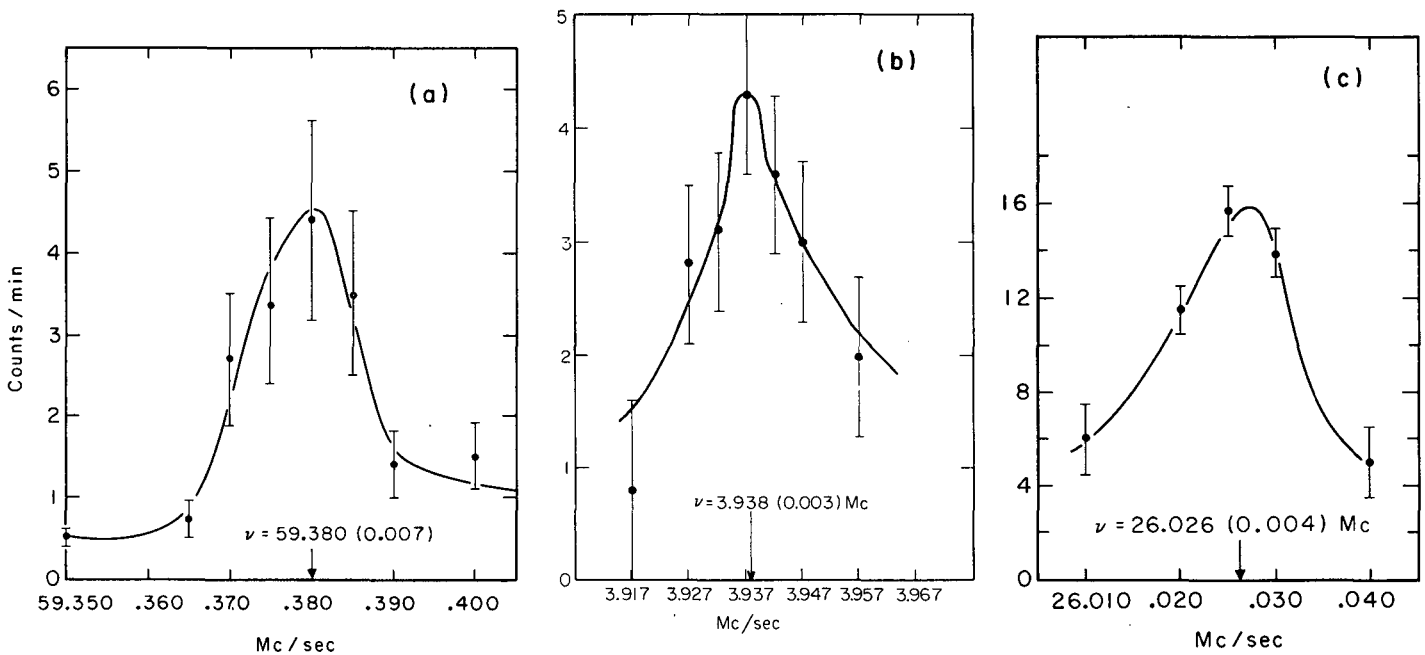

MUB-8152

Fig. 5. Some observed triple-resonance lines in Re.

(a) Re^{188}, H = 300G, (7/2, 1/2) ⟷ (5/2, 1/2);

(b) Re^{186}, H = 500G, (5/2, 1/2) ⟷ (3/2, 3/2);

(c) Re^{186}, H = 300G, (5/2, 1/2) ⟷ (3/2, 1/2).

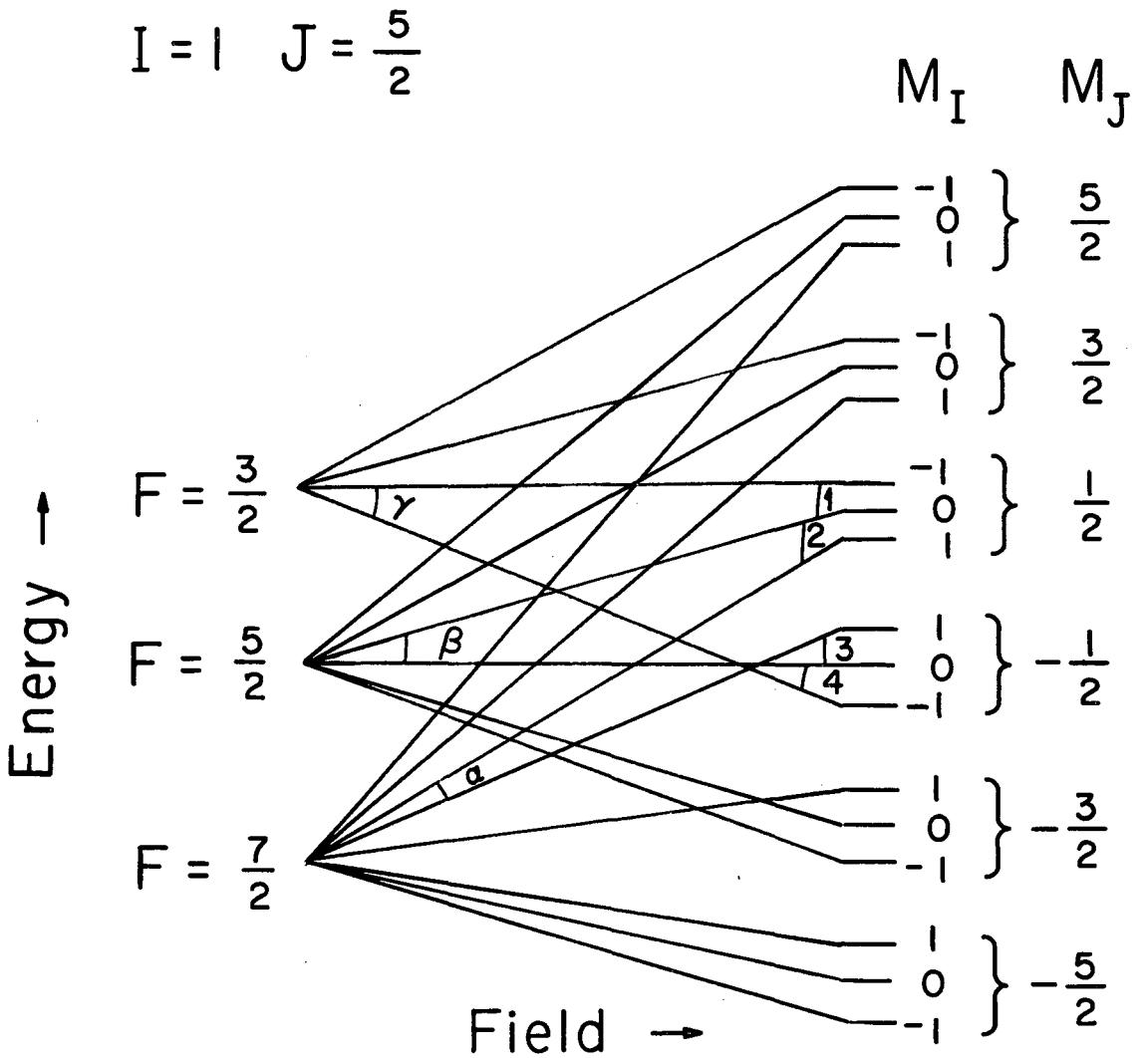

MUB-4244

Fig. 6. Breit-Rabi diagram for Re^{186} and Re^{188}. $I = 1$, $J = 5/2$.

Table II. Re data fit.

Re^{186} Data Fit

A = - 78.3060(.0010) Mc/sec

B = + 8.3595(16) Mc/sec

g_J = - 1.951988(39)

$g_I \times 10^4$ = 9.341(23)

Transition								
F	M_F		F'	M'_F	H (gauss)	Frequency (Mc/sec)	Residual (Mc/sec)
7/2	1/2	⟷	5/2	-1/2	199.9229	24.735(5)	0.0002
3/2	-3/2	⟷	5/2	-1/2	299.8773	16.647(6)	0.002
3/2	-1/2	⟷	5/2	1/2	299.9612	59.380(5)	0.008
7/2	1/2	⟷	5/2	-1/2	299.8598	3.169(4)	- 0.003
3/2	-1/2	⟷	5/2	1/2	399.7824	54.343(4)	- 0.001
3/2	-3/2	⟷	5/2	-1/2	399.7974	22.334(4)	- 0.004
7/2	1/2	⟷	5/2	-1/2	399.8003	6.936(4)	- 0.003
3/2	-1/2	⟷	5/2	1/2	499.8241	51.064(3)	- 0.002
3/2	-3/2	⟷	5/2	-1/2	499.8241	26.026(3)	0.001

Re^{188} Data Fit

A = - 80.4326(8) Mc/sec

B = + 7.7463(11) Mc/sec

g_J = - 1.952072(60)

$g_I \times 10^4$ = 9.607(.029)

Transition								
F	M_F		F'	M'_F	H (gauss)	Frequency (Mc/sec)	Residual (Mc/sec)
7/2	1/2	⟷	5/2	-1/2	99.9675	92.755(3)	- 0.0004
3/2	-1/2	⟷	5/2	1/2	299.8889	61.835(1)	0.0003
3/2	-3/2	⟷	5/2	-1/2	299.8819	15.895(2)	0.001
7/2	1/2	⟷	5/2	-1/2	299.8714	3.938(1)	0.00008
3/2	-3/2	⟷	5/2	-1/2	399.7780	21.837(2)	0.0002

Fit to the observed triple resonances according to the Hamiltonian

$$A\bar{I}\cdot\bar{J} + B\frac{1}{2IJ(2I-1)(2J-1)}\left[3(\bar{I}\cdot\bar{J})^2 + 3/2(\bar{I}\cdot\bar{J}) - I(I+1)J(J+1)\right] - g_J\mu_0\bar{J}\cdot\bar{H} - g_I\mu_0\bar{I}\cdot\bar{H}.$$

The magnetic moment of Re^{185} has been measured to be $\mu_I = +3.144$ nm,[19] and the dipole constant has been measured to be $A(185) = -72(24)$ Mc/sec.[20] These two measurements, in conjunction with our measurement showing that $\mu_I(186)$ and $\mu_I(188)$ are positive, unambiguously determine the sign of both A(186) and A(188) to be negative.

The hyperfine anomaly is given by

$$^{186}\Delta^{188} = \frac{A^{186}/A^{188}}{g_I^{186}/g_I^{188}} - 1 = 0.1(0.4)\%.$$

The values of g_I should be corrected for diamagnetic shielding,[21] i.e.,

$$g_I = g_I^{\text{measured}} \frac{1}{1 - \sigma} .$$

We can use $1/(1 - \sigma) = 1.00714$, the value for $Z = 64$. Then

$$g_I(186) = 9.41(2) \times 10^{-4}$$

$$\mu_I(186) = 1.728(3) \text{ nm}$$

$$g_I(188) = 9.68(3) \times 10^{-4}$$

$$\mu_I(188) = 1.777(5) \text{ nm}.$$

A weighted mean of the two values of g_J is

$$g_J(^6S_{5/2}) = -1.952021(33).$$

C. Second-Order Effects

There are two types of second-order effects, caused by mixing in of higher J states, which can affect the results of this experiment. These types are corrections to g_I, which directly affect our results, and corrections to A, which affect the measured anomaly.

It is possible to obtain an approximate upper limit for the effect without embarking on the detailed analysis outlined in Sec. II. C. Thus for corrections to g_I, we can evaluate

$$g'_I \mu_0 H \approx \frac{2W_{hfs} W_{mag}}{E_J - E'_J} ,$$

where W_{hfs} is the energy due to terms linear in A and B (evaluated in the IM_IJM_J representation) of a $\Delta M_I = \pm 1$, $\Delta M_J = 0$ transition

$$W_{hfs} = AM_J + \frac{B[3M_J^2 - J(J+1)]\,3[M_I^2(1) - M_I^2(2)]}{4(J)(2J-1)(I)(2I-1)} .$$

Here W_{mag} is just $g_J\mu_0 HM_J$, and g_I' is the spurious g_I term. The first excited J state in the ground configuration of Re lies approximately 14,000 cm^{-1} above the ground level.[22] Then

$$g_I' \approx \frac{(2)(80)(2)\frac{1}{2} \times 10^6}{4.2 \times 10^{14}} \approx 4 \times 10^{-7},$$

which is an order of magnitude smaller than the uncertainty in g_I. At 500 G, this would correspond to a shift in frequency of 0.3 kc, which would be completely undetectable.

In like manner, we can obtain an order-of-magnitude estimate of the error in A:

$$A' \approx \frac{[A(I\cdot J)]^2}{E_J - E_J'}$$

$$\approx \frac{4(80\cdot 80) \times 10^6}{4.2 \times 10^{14}} \approx 6.0 \times 10^{-5} \text{ Mc/sec.}$$

This, of course, is also negligibly small.

Another possible source of error in our measurement arises from the well-known Bloch-Seigert[23, 2] effect. When two oscillating frequencies are present simultaneously, as they are in this experiment, resonance frequencies are shifted by an amount

$$\Delta\omega = \frac{\omega_0}{(\omega_0 - \omega_1)^2} ,$$

where ω_0 is the frequency of the transition being observed, and ω_1 is the other frequency. In this case ω_0 corresponds to the C transition, typically of the order of 50 Mc/sec; and ω_1 is the A or B transition frequency, typically of the order of 1000 Mc/sec. Then

$$\Delta\omega \approx \frac{50}{(10^3)^2} = 5\times 10^{-5} \text{ Mc/sec},$$

which is 1/500th a C resonance line width.

D. Hyperfine Fields

Trees[18] has shown that in Re the $^6S_{5/2}$ ground state is not pure but contains components due both to the breakdown of L and S and to admixing of the configuration $(5d)^6(6s)$ into the ground configuration $(5d)^5(6s)^2$. Trees gives as the ground-state wavefunction[18]

$\Psi(J = 5/2) =$

$$\sqrt{0.874}\,|^6S_{5/2}\rangle - \sqrt{0.108}\,|^4P_{5/2}\rangle + \sqrt{0.006}\,|^4D_{5/2}\rangle + \sqrt{0.003}\,|(4^3P)^4P_{5/2}\rangle$$

$$- \sqrt{0.005}\,|5^2D_{5/2}\rangle - \sqrt{0.003}\,|1^2D_{5/2}\rangle + \sqrt{0.001}\,|3^2F_{5/2}\rangle \; .$$

The calculation of the magnetic field at the nucleus B_z

$$B_z = -\frac{2\mu_0}{r^3}\sum_i \left[\ell_{iz} - \sqrt{10}\,(\sigma C^2)_i^{\;1}_{\;0}\right]$$

and the gradient of the electric field at the nucleus q_J

$$q_J = \frac{1}{r^3}\sum_i (3\cos^2\theta - 1)_i$$

can be carried out by expanding the wavefunctions above into sums of determinantal product states. This method is straightforward and is described in detail in Condon and Shortley.[24] The important terms in the evaluation of B_z and q_J, when $\Psi(5/2)$ is used, will, because of the size of the coefficients in $\Psi(5/2)$, obviously arise from elements diagonal in $|^6S\rangle$ and $|^4P\rangle$ and from off-diagonal elements depending on $|^6S\rangle$. However, B_z and q_J can only connect states with $\Delta L = 0, \pm 1, \pm 2$, $\Delta S = 0, \pm 1$. These criteria mean that only the first four states in $\Psi(5/2)$ will be important. The first three of these are given by

$$|^6S_{5/2}\,5/2\rangle = (2^+\,1^+\,0^+\,-1^+\,-2^+)$$

$$|^4P_{5/2}\,5/2\rangle = \frac{1}{\sqrt{30}}\,(3A + \sqrt{6}\,B + \sqrt{6}\,C + 3D)$$

$$|^4D_{5/2}\,5/2\rangle = \frac{1}{\sqrt{7}}\left[\sqrt{2/7}\,(A + \sqrt{6}\,B - \sqrt{6}\,C - D) + \frac{1}{\sqrt{14}}\left\{\sqrt{6}(E + F + G) + 2(H + I + J + K + L + M)\right\}\right] ,$$

where

$A = 2^+\,1^+\,0^+\,0^-\,-2^+$ $\qquad$ $H = 2^-\,1^+\,0^+\,0^-\,-1^+$

$B = 2^+\,1^+\,0^+\,-1^+\,-1^-$ $\qquad$ $I = 2^+\,1^-\,0^+\,0^-\,-1^+$

$C = 2^+\,2^-\,0^+\,-1^+\,-2^+$ $\qquad$ $J = 2^+\,1^+\,0^+\,0^-\,-1^-$

$D = 2^+\,1^+\,1^-\,-1^+\,-2^+$ $\qquad$ $K = 2^+\,2^-\,1^-\,-1^+\,-2^+$

$E = 2^-\,1^+\,1^-\,0^+\,-2^+$ $\qquad$ $L = 2^+\,2^-\,1^+\,-1^-\,-2^+$

$F = 2^+\,1^+\,1^-\,0^-\,-2^+$ $\qquad$ $M = 2^+\,2^-\,1^+\,-1^+\,-2^-$.

$G = 2^+\,1^+\,1^-\,0^+\,-2^-$

The fourth term $|(4^3P)^4P\rangle$ is in the configuration $(5d)^6 6s$. The six d electrons couple to a ^3P state of seniority 4, which then couples to the s electron to form a 4p state. The $|4^3P\rangle$ state is most easily formed by first constructing a $|d^4\,{}^3P\rangle$ state of seniority 4 and then multiplying it by a $|d^2\,{}^1S\rangle$ state. The resulting sum will naturally have many states that must be dropped because they are forbidden by the Pauli principle, and many that are not in standard order as defined by Condon and Shortley.[24] The result is that

$$|4^3P_2\,2\rangle = \frac{1}{4\sqrt{105}}\left[4\sqrt{6}\,A' - 16B' - 4C' + 4\sqrt{6}\,D' - 6\sqrt{6}\,E' - 6\sqrt{6}\,F' + 8\sqrt{6}\,G' + 20H'\right] ,$$

where

$$A' = 2^+ 2^- 1^+ 0^+ -2^+ -2^- \qquad E' = 2^+ 1^+ 1^- 0^+ -1^- -2^+$$

$$B' = 2^+ 2^- 0^+ 0^- -1^+ -2^+ \qquad F' = 2^+ 1^+ 1^- 0^- -1^+ -2^+$$

$$C' = 2^+ 2^- 1^+ -1^+ -1^- -2^+ \qquad G' = 2^- 1^+ 1^- 0^+ -1^+ -2^+$$

$$D' = 2^+ 1^+ 1^- 0^+ -1^+ -2^- \qquad H' = 2^+ 1^+ 0^+ 0^- -1^+ -1^- \ .$$

Then $\left|(4^3P)^4P_{5/2}\ 5/2\right\rangle = \left|4^3P_2\ 2\right\rangle \left|^2S_{1/2}\ 1/2\right\rangle$. This state is, of course, important because of its contribution to A due to its unpaired s electron [Eq. (28)].

The states constructed in this manner are unique to within a phase factor. That is, when constructing a state orthogonal to ψ_a, one can use either $+\psi_b$ or $-\psi_b$. In order to assure that our phase convention is consistent with that of Trees,[18] we have evaluated the coefficients in $\Psi(5/2)$ according to perturbation theory. The perturbing term that breaks down L and S as good quantum numbers is $\sum_i a_d \ell_i \cdot s_i$, where $a_d > 0$. Then

$$\frac{1}{E_{^6S} - E_{^4P}} \left\langle {}^6S_{5/2}\ 5/2 \middle| \sum_i \ell_i \cdot s_i \middle| {}^4P_{5/2}\ 5/2 \right\rangle = \frac{\sqrt{5}}{E_{^6S} - E_{^4P}} < 0 \ ,$$

showing that $\left|{}^4P_{5/2}\right\rangle$ has been constructed to agree with Trees' notation. Second-order theory is required for the $\left|{}^4D_{5/2}\right\rangle$ term, since $\sum \ell_i \cdot s_i$ can change L by only ± 1.

$$\frac{\left\langle {}^6S_{5/2}\ 5/2 \middle| \sum_i \ell_i \cdot s_i \middle| {}^4P_{5/2}\ 5/2 \right\rangle \left\langle {}^4P_{5/2}\ 5/2 \middle| \sum_i \ell_i \cdot s_i \middle| {}^4D_{5/2}\ 5/2 \right\rangle}{(E_{^6S} - E_{^4D})\ (E_{^6S} - E_{^4P})}$$

$$= \frac{\sqrt{15}}{5(E_{^6S} - E_{^4P})(E_{^6S} - E_{^4D})} > 0,$$

confirming the phase assignment of ${}^4D_{5/2}$. The final term $\left|(4^3P)^4P_{5/2}\right\rangle$ is important only in diagonal matrix elements, so the phase is of no real importance.

In order to evaluate B_z and q_J one needs to know the two radial parameters $\langle 1/r^3 \rangle_{5d}$ and $|\Psi(0)|^2_{6s}$. Cohen[25] has calculated Hartree solutions to the Dirac equation for the ground states of tungsten (Z = 74) and platinum (Z = 78). Utilizing the discussion of Sec. II. B, one can write

$$\langle 1/r^3 \rangle_{\text{dipole}} = \frac{2}{\alpha a_0(\ell+1)} \int_0^\infty \frac{FG}{r^2}\, dr$$

$$\langle 1/r^3 \rangle_{\text{quad}} = \int_0^\infty \frac{F^2 + G^2}{r^3}\, dr.$$

These equations were evaluated for W and Pt, and a linear interpolation was made to Re(Z = 75). These values are given in Table III.

The value of $|\Psi(0)|^2$ can be obtained from Cohen's functions by means of the equation

$$|\Psi(0)|^2 = -\frac{1}{\pi\alpha a_0} \int \frac{FG}{r^2}\, dr$$

which can be obtained from (59). This equation was also evaluated for W and Pt and a linear interpolation made; results are shown in Table III.

A check on this last value can be obtained by looking at the optical data of Schuler and Korsching[26] on Re^{187}. They have measured the hyperfine structures of the states $^8P_{7/2}$ and $^8P_{5/2}$ in the configuration d^5sp, obtaining $A(^8P_{7/2}) = 113.46$ mK and $A(^8P_{5/2}) = 109.96$ mK. Assuming that d^5 couples to $^6S_{5/2}$, which then couples to the s $^2S_{1/2}$ and the p $^2P_{3/2}$ to form a $|^8P_{9/2}\ 9/2\rangle$ state, we can write

$$|^8P_{7/2}\ 7/2\rangle = 1/\sqrt{9}\Big\{1/\sqrt{2}\Big[\sqrt{5}\,|5/2\ 3/2\rangle\,|1/2\ 1/2\rangle\,|3/2\ 3/2\rangle + |5/2\ 5/2\rangle\,|1/2\ -1/2\rangle\,|3/2\ 3/2\rangle\Big] - \sqrt{6}\,|5/2\ 5/2\rangle\,|1/2\ 1/2\rangle\,|3/2\ 1/2\rangle\Big\}$$

and

$$|^8P_{5/2}\ 5/2\rangle = 1/60\sqrt{60/7}\Big\{\sqrt{30}\,|5/2\ 1/2\rangle\,|1/2\ 1/2\rangle\,|3/2\ 3/2\rangle + \sqrt{15}\,|5/2\ 3/2\rangle\,|1/2\ -1/2\rangle\,|3/2\ 3/2\rangle - 5\sqrt{5}\,|5/2\ 3/2\rangle\,|1/2\ 1/2\rangle\,|3/2\ 1/2\rangle - 5\,|5/2\ 5/2\rangle\,|1/2\ -1/2\rangle\,|3/2\ 1/2\rangle + 15\,|5/2\ 5/2\rangle\,|1/2\ 1/2\rangle\,|3/2\ -1/2\rangle\Big\},$$

Table III. Re numerical parameters (in units of a_0^{-3}).

	W^a	Pt^a	Re^b
$\langle 1/r^3 \rangle_{5d}^{dipole}$	4.7	10.0	6.0
$\langle 1/r^3 \rangle_{5d}^{quadrupole}$	5.1	11.1	6.6
$\lvert\Psi(0)\rvert_{6s}^2$	19.7	24.7	20.9
$e\int_0^\infty \frac{F_- G_-}{r^2}\,dr$	14.0 μ_0	29.7 μ_0	17.9 μ_0
$e\int_0^\infty \frac{F_+ G_+}{r^2}\,dr$	---	- 16.0 μ_0	- 9.6 μ_0
$e\int_0^\infty \frac{F_+ G_- + F_- G_+}{r^2}\,dr$	---	8.6 μ_0	5.2 μ_0
$\int_0^\infty \frac{F_-^2 + G_-^2}{r^3}\,dr$	5.1	11.1	6.6
$\int_0^\infty \frac{F_+^2 + G_+^2}{r^3}\,dr$	---	8.3	5.0
$\int_0^\infty \frac{F_+ F_- + G_+ G_-}{r^3}\,dr$	---	9.0	5.4

a. These are evaluated from Cohen's wave functions of W and Pt.

b. The values for Re are obtained by linear interpolation.

where we have written $|^6S_{5/2}\ m\rangle$ as $|5/2\ m\rangle$, etc. The measured A values in this configuration will be almost totally due to the unpaired s electron; assuming that this is the total contribution, one obtains

$$A(^8P_{7/2}) = \frac{8}{9}\ \frac{a_{6s}}{7}$$

$$A(^8P_{5/2}) = \frac{17}{15}\ \frac{a_{6s}}{7}\ ,$$

where a_{6s} is given by Eq. (28). The disagreement between the ratio of these two A values with the ratio of the experimental values indicates that the simple coupling scheme is not completely correct. However, the calculated values, like the experimental values, are nearly the same. Other coupling schemes also lead to values of approximately $a_{6s}/7$ for both J states. Assuming that $A(^8P_{7/2}) = A(^8P_{5/2}) = a_{6s}/7$, we obtain $a_{6s} \approx 0.8$ mK, to be compared with a value of $a_{6s} = 0.7$ mK that would be obtained using $|\Psi_0|^2$ as given by Cohen's data.

Evaluation of B_z and q_J then proceeds in a straightforward manner, and one obtains

$$A = +\ 44.8\ \mu_I\ \text{Mc/sec} = +\ 78.4\ \text{Mc/sec}$$

$$B = +\ 33.0\ Q\ \text{Mc/sec.}$$

The contributions to these quantities from the various matrix elements are shown in Table IV.

The magnitude of A is correct, but apparently the sign is wrong. We therefore must consider relativistic effects. Since the non-relativistic treatment is in terms of determinantal wave functions, we shall use the first method discussed in Sec. II. B. 2.

The integrals $\int(F_-G_-/r^2)dr$ and $\int(F_+^2 + G_+^2/r^3)dr$ have been evaluated for both W and Pt by means of Cohen's wavefunctions and linear interpolations made to Re. The values of F_+ and G_+ have not been calculated for W, since the ground state of tungsten has no $5d_{5/2}$ electrons. The Re integrals containing F_+ and G_+ were therefore obtained by scaling down the Pt integrals by the same factor as was used for the integrals in F_- and G_-.

Table IV. Nonrelativistic matrix elements in rhenium.

Dipole elements

$$\langle {}^4P_{5/2}\ 5/2 | H_z | {}^4P_{5/2}\ 5/2 \rangle = -\frac{8}{5}\mu_0 \left\langle \frac{1}{r^3} \right\rangle$$

$$\langle {}^4P_{5/2}\ 5/2 | H_z | {}^6S_{5/2}\ 5/2 \rangle = 0$$

$$\langle {}^4D_{5/2}\ 5/2 | H_z | {}^6S_{5/2}\ 5/2 \rangle = \frac{2\sqrt{12}}{7}\mu_0 \left\langle \frac{1}{r^3} \right\rangle$$

Quadrupole elements

$$\langle {}^4P_{5/2}\ 5/2 | 3\cos^2\theta - 1 | {}^4D_{5/2}\ 5/2 \rangle = -\frac{12}{7}\sqrt{15}$$

$$\langle {}^4P_{5/2}\ 5/2 | 3\cos^2\theta - 1 | {}^4P_{5/2}\ 5/2 \rangle = 0$$

One then obtains a relativistic correction to the nonrelativistic values of

$$A = -83.5\ \mu_I\ \text{Mc/sec} = -146.1\ \text{Mc/sec}$$
$$B = -28.0\ Q\ \text{Mc/sec},$$

giving for the total calculated values

$$A = -38.7\ \mu_I\ \text{Mc/sec} = -67.7\ \text{Mc/sec}$$
$$B = 4.7\ Q\ \text{Mc/sec}.$$

The relativistic matrix elements are shown in Table V, and the various contributions to A and B are collected in Table VI.

The agreement between calculated and experimental values is now fairly good. It is impossible to determine whether the difference between the measured and calculated A values is due to uncertainties in the relativistic parameters or to core polarization.

Comparison of measured and calculated values for B shows that $Q = 1.7$ barns. This implies that Q_0, the nuclear quadrupole moment with respect to the symmetry axis of the nucleus, is $Q_0 = 10\,Q = 17$ barns. If we assume a deformation parameter of $\delta = 0.2$ (see Sec. V.E) for Re, then

$$Q_0 = \frac{4}{5}\ ZR_0^2\delta = 6.0\ \text{barns},$$

which is considerably smaller than the above prediction. This discrepancy could arise either from uncertainties in radial integrals or from quadrupole shielding. Sternheimer[27] has calculated an antishielding factor of $R = -0.51$ for the configuration $(5d)^4$ in tungsten. If this number applies to Re, then

$$Q = 1.7 = Q'(1 - R)$$

$$Q' = \frac{1.7}{1.5} = 1.1,$$

and Q_0 would become 11 barns. In any case, in the region of Re the antishielding factors are of the right sign to bring the two values of Q_0 closer together.

An alternate method of calculating relativistic radial integrals involves use of the Casimir[28] correction factors. Choosing $Z_{eff} = Z - 11 = 64$, and using the $\langle 1/r^3 \rangle$ values used in the nonrelativistic calculations, we obtain relativistic corrections a quarter the size of our previous result. This result, in direct contrast to the

Table V. Relativistic matrix elements in rhenium.

	Dipole elements		
	eP_{++}	eP_{--}	eP_{+-}
$\langle {}^6S_{5/2}\ 5/2 \| H_z \| {}^6S_{5/2}\ 5/2 \rangle$	420/175	80/75	40/25
$\langle {}^4P_{5/2}\ 5/2 \| H_z \| {}^4P_{5/2}\ 5/2 \rangle$	11088/5250	1392/2250	576/750
$\langle {}^6S_{5/2}\ 5/2 \| H_z \| {}^4P_{5/2}\ 5/2 \rangle$	0	0	0
$\langle {}^6S_{5/2}\ 5/2 \| H_z \| {}^4D_{5/2}\ 5/2 \rangle$	$-168/175\sqrt{12/49}$	$-112/75\sqrt{12/49}$	$14/25\sqrt{12/49}$
	Quadrupole elements		
	R_{++}	R_{--}	R_{+-}
$\langle {}^6S_{5/2}\ 5/2 \| \frac{(3\cos^2\theta - 1)}{r^3} \| {}^6S_{5/2}\ 5/2 \rangle$	0	0	0
$\langle {}^4P_{5/2}\ 5/2 \| \frac{(3\cos^2\theta - 1)}{r^3} \| {}^4P_{5/2}\ 5/2 \rangle$	0	0	0
$\langle {}^4P_{5/2}\ 5/2 \| \frac{(3\cos^2\theta - 1)}{r^3} \| {}^4D_{5/2}\ 5/2 \rangle$	$624/1225(1/\sqrt{15})$	$42/175(1\sqrt{15})$	$3546/3675(1/\sqrt{15})$
$\langle {}^6S_{5/2}\ 5/2 \| \frac{(3\cos^2\theta - 1)}{r^3} \| {}^4P_{5/2}\ 5/2 \rangle$	$112/175(1\sqrt{5})$	$-4/25(1\sqrt{5})$	$-252/525(1/\sqrt{5})$

Table VI. Contribution to the hyperfine constants A and B in rhenium.

Source	Magnitude	
	A (Mc/sec)	B (Mc/sec)
Breakdown of LS coupling within $(5d)^5(6s)^2$	$33.6\ \mu_I$ [a]	$+\ 33.0\ Q$ [b]
Configuration mixing $(5d)^6(6s)$	$11.2\ \mu_I$	$-\ 0.3\ Q$
Relativistic corrections	$-\ 83.5\ \mu_I$	$-\ 28.0\ Q$
Total calculated	$-\ 38.7\ \mu_I$	$4.7\ Q$
Total experimental	$-\ 46.0\ \mu_I$	8.0

a. μ_I in nm.

b. Q in barns.

earlier one, is insufficient to explain the experimental results. For this reason, we believe the Casimir factors are only a quarter as big as they should be for d electrons. This result is not surprising, since Schwartz[29] showed that the Casimir factors were accurate, but fortuitously so, for p electrons; and Sandars[30] has shown them to be only a tenth as big as they should be for f electrons.

E. Nuclear Structure

Mottelson and Nilsson[31] have calculated equilibrium values of the deformation parameter δ for odd A nuclei in the region $151 < A < 195$, using the collective model with a harmonic-oscillator single-particle potential. Experimental values of δ were then obtained from values of Q_0 based on observed E2 transition probabilities. Agreement between calculated and measured δ's for both odd-A and even-even nuclei is good over most of the region, particularly for $_{74}W$ and $_{76}Os$.

The predicted value of δ for $_{75}Re$ is 0.19, which agrees favorably with the value 0.22 obtained from the measured quadrupole moment of Re^{185}. This δ and the measured ground-state spins of 5/2+ for both Re^{185} and Re^{187} led to the assignment of [402]5/2 to the 75th proton.

Because both Re^{186} and Re^{188} have I = 1-, the 111th and 113th neutrons have been assigned to the [512]3/2 state. This assignment fits the Mottelson-Nilsson energy-level diagram exactly if $\delta_{186} > 0.22$, and $0.19 < \delta_{188} < 0.22$. The ordering $\delta_{188} < \delta_{186}$ is supported by the results of our experiment. The quadrupole constants B are a measure of the deformation, and $B_{188} < B_{186}$ implies that $\delta_{188} < \delta_{186}$. For the proposed state assignments, an increasing nuclear moment implies smaller deformation (see Table VII). Therefore, the results $\mu_I(188) > \mu_I(186)$ supports the conclusion $\delta_{188} < \delta_{186}$.

The magnetic moment μ_I has been calculated with these state assignments and the wave functions of Nilsson and Mottelson. We calculated this moment for various positive values of δ, with both free nucleon g factors and the quenched g factors ($g_{sp} = 4.0$, $g_{sn} = -2.4$) suggested by Chiao.[32] The results are shown in Table VII. The value Z/A was used for the core g factor, g_R. Chiao has suggested, on the basis of different pairing energies for neutrons and protons, that g_R

Table VII. Nuclear moments calculated with Nilsson wave functions.[a]

	η		
	2	4	6
Free-nucleon g factors	2.11	1.92	1.84
Quenched-nucleon g factors	1.89	1.77	1.72

a. Proton state [402↑] (5/2+). Neutron state [512↓] (3/2-).

for odd-odd nuclei should be $g_R = 3/4\ Z/A$. If this value were used, each of the results in Table VII would be lowered by 0.05 nm.

Table VII shows that when quenched g factors are used, $\mu_I(188)$ is predicted very well by a deformation of 0.2, and $\mu_I(186)$ by a deformation of slightly less than 0.3. This is in good agreement with the deformations assumed.

VI. AMERICIUM

A. Introduction

The research on americium, like that on rhenium, was undertaken primarily for two reasons. First, americium, like rhenium, has an $L = 0$ ground state arising from a half-filled shell; in this case, the ground state is $(5f)^7(6s)^2\ {}^8S_{7/2}$. Second, because the two isotopes studied, Am^{241} and Am^{242}, have very different nuclear structures according to the Nilsson model, it is interesting to study the effects caused by such a difference.

Marrus, Nierenberg and Winocur[33] have measured g_J, A, and B of both Am^{241} and Am^{242}. They also found that there was a breakdown of LS coupling in the ground state of Am, and obtained a wavefunction for this state.

B. Experimental Methods and Results

Americium-241 in an HCl solution was obtained from the stockpile of the Lawrence Radiation Laboratory group headed by Burris Cunningham. Americium oxide was made from the solution by adding NH_4OH and heating the precipitate $[Am(OH)_3]$ in a furnace until oxidation occurred.

The atomic-beam oven used was of Ta, with a Ta inner liner. The americium oxide, together with an excess of lanthanum metal, was placed in the oven. When the oven was heated to approximately 1000°C, the lanthanum reduced the Am_2O_3 to Am metal. The reduction proceeded very slowly, however, requiring several hours. Despite several efforts, we never observed the rapid reduction in a molybdenum oven described by Winocur[34]. The difference in results was assumed to be caused by differences in impurities in the samples used.

The experimental method used was identical to that used on rhenium. Signal-to-noise ratios of 3:1 were obtainable with the hairpins singly and also with all three hairpins together. The hyperfine levels of Am^{241} ($I = 5/2$) and Am^{242} ($I = 1$) are shown schematically in Figs. 7 and 8, respectively. The A and B

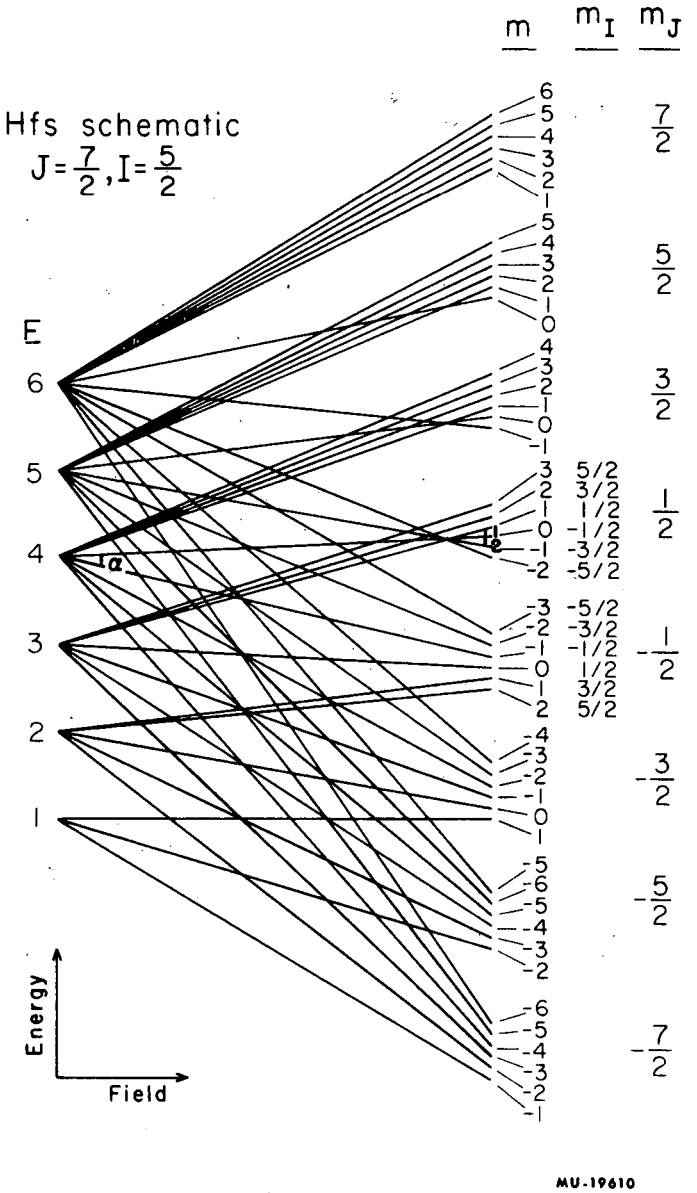

Fig. 7. Breit-Rabi diagram for Am^{241}. I = 5/2, J = 7/2.

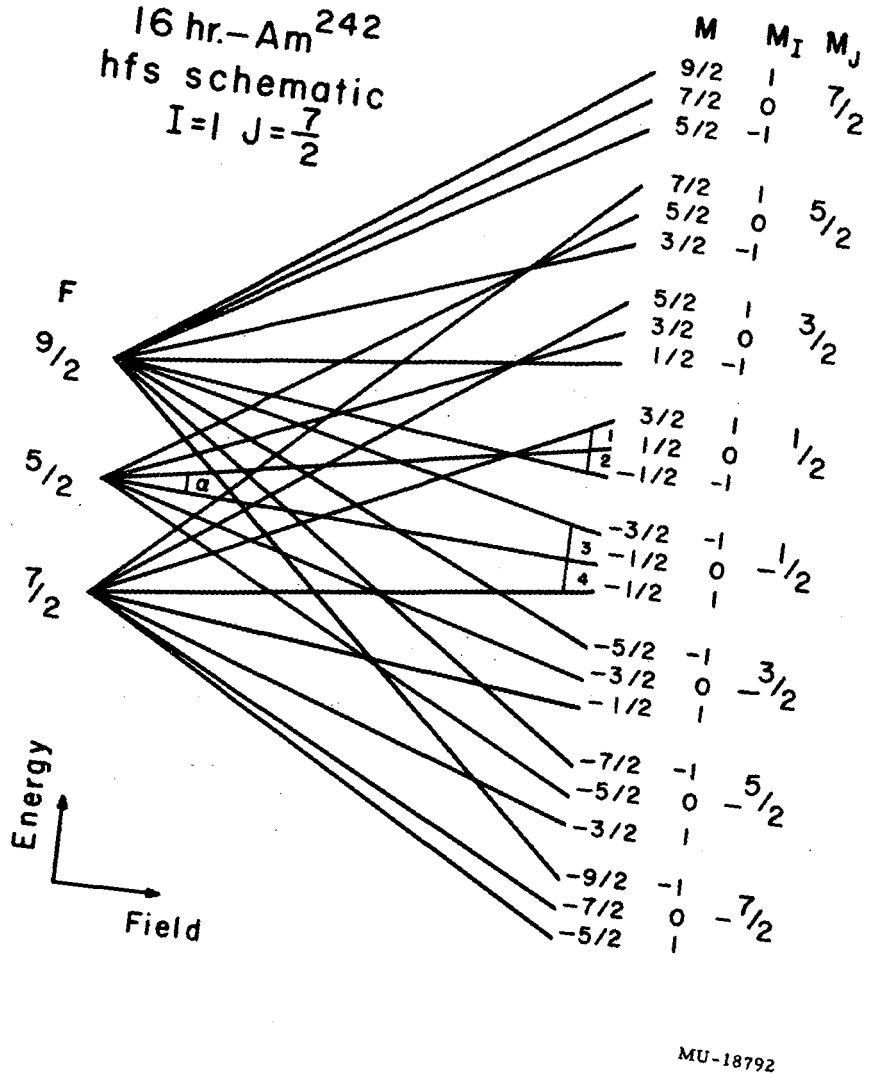

Fig. 8. Breit-Rabi diagram for 16-h Am^{242}. I = 1, J = 7/2.

hairpins were set on the resonances labeled α, the C hairpin on the resonances labeled by Arabic numerals. Some observed triple-resonance lines are shown in Fig. 9.

The Am^{242} data, which consist of one high-field single-hairpin transition and six triple-loop transitions, were combined with that of Marrus et al.[33] for the purpose of data reduction. The data were fitted to a Hamiltonian of the form of Eq. (96), and A, B, g_J, and g_I were varied.

We encountered difficulty in observing high-field α transitions in Am^{241} at the frequencies predicted on the basis of the results of Marrus et al.[33] Observation of a low-field direct transition confirmed Marrus's value of A and B. When these values of A and B, and g_J of Am^{242} were used to predict resonance frequencies, high-field α transitions were observed. The data obtained in this experiment, one direct transition and six triple-loop transitions, were combined with Marrus's direct-transition data for data reduction. These combined data were also fitted to a Hamiltonian of the form of Eq. (96), but this time only A, B, and g_I were varied, with g_J fixed at the value of g_J found in Am^{242}.

Final results were (Table VIII):

$$\left.\begin{aligned} A &= \pm\ 17.1437\ (0.0028)\ \text{Mc/sec} \\ B &= \mp\ 123.8477\ (0.0323)\ \text{Mc/sec} \\ g_I &= +\ 3.42\ (0.06) \times 10^{-4} \end{aligned}\right\}\ Am^{241}$$

$$\left.\begin{aligned} A &= \pm\ 10.1282\ (0.0014)\ \text{Mc/sec} \\ B &= \pm\ 69.6339\ (0.0013)\ \text{Mc/sec} \\ g_J &= -\ 1.937884\ (0.000067) \\ g_I &= +2.059\ (0.008) \times 10^{-4} \end{aligned}\right\}\ Am^{242}$$

This leads to a hyperfine anomaly of

$$^{241}\Delta^{242} = 1.7\ (2.0)\%.$$

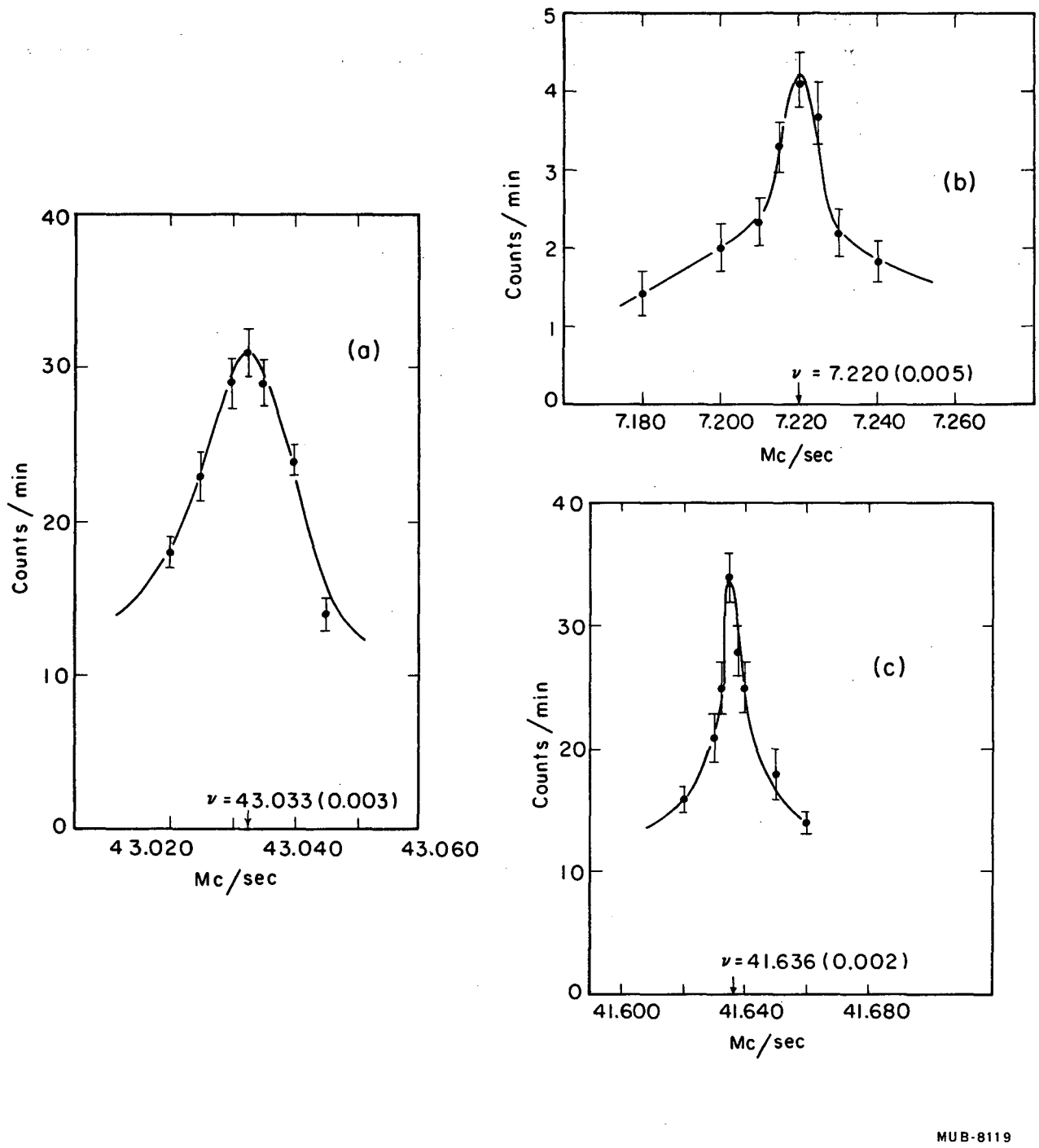

Fig. 9. Some observed triple-resonance lines in Am.

(a) Am^{242}, H = 700G, (2.5, -0.5) ⟷ (3.5, 0.5);

(b) Am^{241}, H = 180G, (3.0, 1.0) ⟷ (4.0, 0.0);

(c) Am^{242}, H = 700G, (2.5, 0.5) ⟷ (4.5, -0.5).

Table VIII. Americium-data fit.

Am^{241}

A = ± 17.1437(28) Mc/sec

B = ∓123.8477(323) Mc/sec

$g_I \times 10^4$ = 3.425(57)

Transition					H (gauss)	Frequency (Mc/sec)	Residual (Mc/sec)
F	M_F		F'	M'_F			
6/2	2/2	↔	8/2	0/2	71.5736	4.870(15)	- 0.00233
10/2	- 2/2	↔	8/2	0/2	71.5736	14.520(25)	- 0.01042
6/2	2/2	↔	8/2	0/2	179.9427	7.220(6)	- 0.00322
10/2	- 2/2	↔	8/2	0/2	179.9473	8.225(7)	0.00240
6/2	2/2	↔	8/2	0/2	449.8825	7.827(6)	0.00204
10/2	- 2/2	↔	8/2	0/2	449.8677	6.290(6)	0.00008
10/2	- 2/2	↔	8/2	- 2/2	2.7993	81.491(7)	0.00007

Am^{242}

A = ± 10.1282(14) Mc/sec

B = ± 69.6339(13) Mc/sec

g_J = - 1.937884(67)

$g_I \times 10^4$ = 2.059(8)

Transition					H (gauss)	Frequency (Mc/sec)	Residual (Mc/sec)
F	M_F		F'	M'_F			
5/2	1/2	↔	5/2	- 1/2	300.0164	815.245(30)	- 0.00241
5/2	1/2	↔	7/2	3/2	299.9033	35.704(5)	0.00034
5/2	1/2	↔	9/2	- 1/2	299.8955	40.934(3)	- 0.00153
5/2	1/2	↔	9/2	- 1/2	699.8325	41.636(2)	0.00011
5/2	1/2	↔	7/2	3/2	699.8162	33.932(2)	- 0.00054
5/2	- 1/2	↔	7/2	1/2	699.8180	43.032(3)	0.00111
5/2	- 1/2	↔	9/2	- 3/2	699.8144	30.487(2)	0.00037

Correcting the values of g_I for diamagnetic shielding and using the value of σ corresponding to $Z = 65$ gives

$$g_I(241) = +3.45\ (0.06) \times 10^{-4}$$
$$\mu_I(241) = +1.58\ (0.03)$$
$$g_I(242) = +2.074\ (0.008) \times 10^{-4}$$
$$\mu_I(242) = +0.3808\ (0.0015).$$

Because both measured μ_I's have the same sign, both values of A must also have the same sign.

C. Second-Order Effects

An upper limit to the second-order corrections to g_I and A can be obtained as in Sec. V.C. The first excited states of Am lie more than 15,000 cm^{-1} above the ground state.[35] Then

$$g_I' \approx \frac{2 \cdot 80 \cdot 2 \times 10^6}{4.5 \times 10^{14}} \approx 7 \times 10^{-7}.$$

Because this is of the same order as the uncertainty in g_I, a more thorough analysis is called for. Equation (67) shows, however, that there are no second-order corrections to g_I if the ground state is pure $^8S_{7/2}$. This is so because, due to $\sum_i \ell_i + 2s_i$, the perturbation term is diagonal in L and S; the admixed J state, J', must therefore be formed by coupling ^8S to a J other than 7/2--this is impossible. As we shall see in Sec. VI. D. the ground state is not pure $^8S_{7/2}$, but has small amounts of $^6P_{7/2}$ and $^6D_{7/2}$ mixed in. An important feature of the half-filled shell is that all diagonal matrix elements of the quadrupole operator are zero. This feature, plus the fact that the perturbation term is diagonal in L and S, means that the large quadrupole-interaction constant can have no second-order effects even in an impure ground state. The dipole interaction, however, can produce second-order effects in an impure ground state, and an estimate of the upper limit to this effect is given by

$$g_I' \approx (0.3)\,\frac{2\cdot 17\cdot \frac{1}{2}\cdot 2\times 10^6}{4.5\times 10^{14}} \approx 2\times 10^{-8}\,,$$

where 0.3 is the fraction of the ground state composed of ^6P and ^6D. This number is less than a tenth the uncertainty in g_I, and shows that second-order perturbations do not measurably influence the value of g_I.

An upper limit to the error in A will be

$$A' \approx \frac{(\Delta\nu)^2}{E_J - E_J'}$$

$$\approx \frac{(90)^2\times 10^6}{4.5\times 10^{14}} \approx 2\times 10^{-5}\ \text{Mc/sec.}$$

This, too, is negligibly small.

D. Hyperfine Fields

Marrus et al.[33] have shown that there is a breakdown of LS coupling in Am. The wavefunction they give for the ground state is

$$\psi(J = 7/2) = 0.882\,|^8S_{7/2}\rangle + 0.457\,|^6P_{7/2}\rangle - 0.114\,|^6D_{7/2}\rangle\,,$$

where the phases have been fixed to agree with Racah's[36] conventions. On the basis of this wavefunction, they calculated the nonrelativistic values of A and B: They found for Am^{241}

$$A = +\ 16.6\ \text{Mc/sec}$$
$$B = +\ 145\ \text{Mc/sec.}$$

These numbers agree in magnitude with the measured values, but the sign of the ratio B/A is wrong. As with the case of Re, the next step was to consider relativistic corrections to A and B.

For calculations in Am, we used the second method discussed in Sec. II. B. 2. Then, from Eq. (51),

$$A = -(0.064)(\alpha - \beta + \gamma) + \alpha + \gamma\left(\frac{0.558}{7}\right).$$

Here 0.558/7 is $-(H_z/2J\mu_0 \frac{1}{r^3})$, with H_z as given by Marrus et al.[33] An error in this paper gives $H_z = -0.41\,\mu_0 \langle 1/r^3 \rangle$ rather than the correct value of $-0.558\,\mu_0 \langle 1/r^3 \rangle$. The relativistic Am wave-functions of Lieberman, Waber, and Cromer[37] were used to evaluate the radial integrals appearing in $\alpha - \beta + \gamma$, α, and γ. These integrals are given in Table IX. Then

$$(\alpha - \beta + \gamma) = 2.353\,\frac{\mu_I \mu_0}{I a_0^3}$$

$$\alpha = -0.147\,\frac{\mu_I \mu_0}{I a_0^3}$$

$$\gamma = 18.286\,\frac{\mu_I \mu_0}{I a_0^3}\,.$$

Using these values, we obtain

$$A = 1.160\,\frac{\mu_I \mu_0}{I a_0^3}$$

giving

$$A(241) = 34.5 \text{ Mc/sec}$$
$$A(242) = 20.8 \text{ Mc/sec.}$$

If we assume that core polarization is responsible for the discrepancy between these numbers and the measured numbers, then

$$\Delta A(241) \approx -17,\ -51 \text{ Mc/sec}$$
$$\Delta A(242) \approx -11,\ -31 \text{ Mc/sec,}$$

where the first number above holds if the measured A's are positive, the second if the A's are negative. It is of value at this point to obtain an estimate of the uncertainty in the radial integrals

Table IX. Am and Pu relativistic radial integrals (in units of a_0^{-3}).

		Am	Pu
$e\int \frac{F_+G_+}{r^2}\,dr$	=	$-23.5\ \mu_0$	$-21.3\ \mu_0$ [a]
$e\int \frac{F_-G_-}{r^2}\,dr$	=	$31.6\ \mu_0$	$28.6\ \mu_0$
$e\int \frac{F_+G_- + F_-G_+}{r^2}\,dr$	=	$6.7\ \mu_0$	$6.1\ \mu_0$ [a]
$\int \frac{F_+^2 + G_+^2}{r^3}\,dr$	=	7.6	
$\int \frac{F_-^2 + G_-^2}{r^3}\,dr$	=	8.6	7.6
$\int \frac{F_+F_- + G_+G_-}{r^3}\,dr$	=	8.2	

a. Obtained by scaling.

used. One parameter closely related to these integrals is ζ, the spin-orbit coupling constant, since all are proportional to $\langle 1/r^3 \rangle$. The difference in energy eigenvalues for $f_{7/2}$ and $f_{5/2}$ electrons should be just $\frac{7}{2}\zeta$; the wavefunctions used then give ζ (Am) = 3020 cm^{-1}. Blume, Freeman, and Watson[38] showed that, in the rare earths, ζ obtained from a Hartree-Fock calculation is decreased by about 10% if two-body interactions such as spin-other-orbit are considered. If such a factor holds for Am, then the value of ζ given by these wavefunctions would be lowered to approximately 2700 cm^{-1}. The correct value of ζ (Am) is approximately 2400 cm^{-1}. An ζ calculated from these wavefunctions would then be about 12% too large.

Foglio and Pryce,[39] from an investigation based on the Thomas-Fermi model, found that in the region of Pu and Am, $\zeta / \langle 1/r^3 \rangle \approx 370\ cm^{-1}/Au$, or $\langle 1/r^3 \rangle = 6.5\ a_0^{-3}$. We can also calculate $\langle 1/r^3 \rangle$ from $\langle 1/r^3 \rangle = \int \frac{F^2 + G^2}{r^3} dr$, obtaining $\langle 1/r^3 \rangle \approx 8.1\ a_0^{-3}$. This is 20% higher than that obtained from the relationship suggested by Foglio and Pryce.

Although there is, unfortunately, no way of estimating whether the ratios of the various radial integrals are in error, it appears that the magnitudes of these integrals may be too high by about 15%. If such is the case, the numbers above for A should be decreased by 15%, with corresponding decreases in ΔA.

We can estimate the amount of core polarization involved in Am by looking at core polarization in Pu. Bauche and Judd[8] investigated core polarization in Pu in the six J levels of ^7F. These levels all have values of g_J lying between - 1.495 and - 1.424, which means, according to (69), that the core polarization should be approximately a constant for all six levels. Then for all levels,

$$A_J(\text{meas}) = A_J(\text{calc}) + \Delta A. \tag{97}$$

Bauche and Judd treated μ_I, in addition to ΔA, as an unknown, so that there were two adjustable parameters in the above equation. With six J states, the parameters were overdetermined. If the various equations of Eq. (97) were consistent, then the straight lines that they define should meet in a point. They found that

$$\Delta A = -15 \pm 9 \text{ Mc/sec}$$

$$\mu_I = 0.17\ (0.04) \text{ nm.}$$

Because their work was done nonrelativistically, ΔA must include both core polarization and relativistic effects. In an effort to separate these effects, we repeated their work calculating A relativistically and using the relativistic Pu wavefunctions of Lieberman et al.[37] Their Pu calculations do not include wavefunctions for an $f_{7/2}$ electron[37]; integrals for $f_{7/2}$ electrons were obtained by scaling down the Am integrals by the ratio of the Pu $f_{5/2}$ integral to the Am $f_{5/2}$ integral. This is equivalent to scaling down the factors $\alpha - \beta + \gamma$, etc. by the same factor, giving

$$\alpha - \beta + \gamma = 2.015 \frac{\mu_I \mu_0}{I a_0^3}$$

$$\alpha = -0.133 \frac{\mu_I \mu_0}{I a_0^3}$$

$$\gamma = 16.570 \frac{\mu_I \mu_0}{I a_0^3}.$$

The resulting calculated values for A are given in Table X, together with the measured values of A. The measured values of A for J from 2 to 6 have an uncertainty of 15 Mc/sec; the magnitude of A for J = 1 is known to 5 kc/sec, but the sign of A is unknown. The nearly horizontal broken lines in Fig. 10 represent this uncertainty in sign for J = 1.

The equation plotted in Fig. 10 is

$$A\,(\text{meas}) = \gamma\Omega + \Delta A,$$

where $\gamma = [A(\text{calc})\, a_0^3 I]/(\mu_I \mu_0)$ and $\Omega = (\mu_I \mu_0 / I a_0^3)\, F$. [F is the scaling factor that varies the magnitude of the radial integrals used in A(calc)]. From the discussion concerning the Am integrals, we would expect F to be less than one.

Comparison of Fig. 10 with the corresponding figure given by Bauche and Judd[8] shows that the lines in our graph meet no more

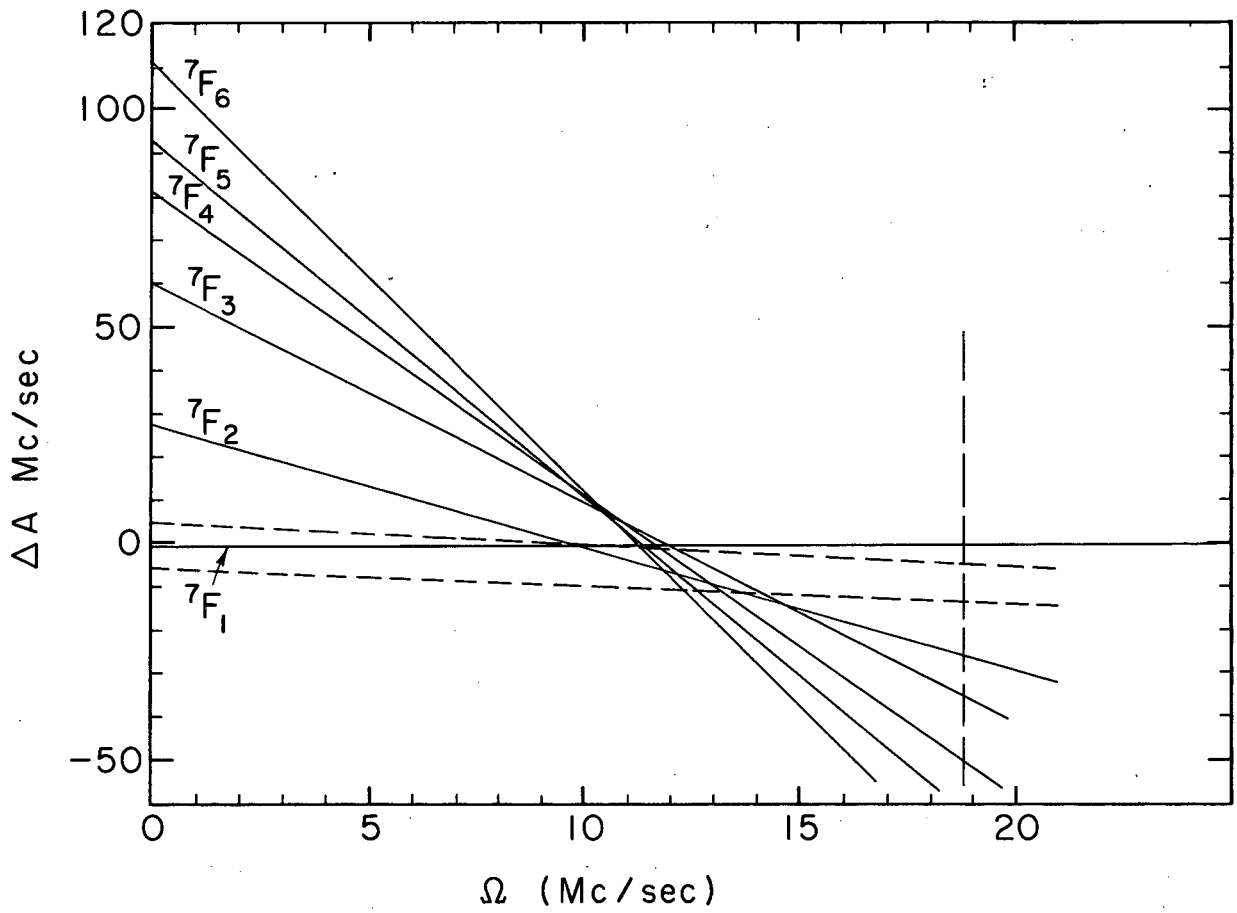

MUB-8118

Fig. 10. Plot of A(meas) = $\gamma\Omega + \Delta A$ for Pu.

Table X. A values of Pu^{239}.

J	A(meas) (Mc/sec)	A(calc) (Mc/sec)
6	111.0	$9.97 \frac{\mu_I \mu_0}{I a_0^3}$
5	93.0	8.27 "
4	81.0	6.94 "
3	60.0	5.04 "
2	27.6	2.84 "
1	± 5.13	0.48 "

nearly in a point than they do in the earlier graph. This is of no real importance because, due to the uncertainty in A for J = 2 to 6, any such meeting would be accidental. The important lines are those corresponding to J = 1, because they have essentially no uncertainty in the ΔA and Ω intercepts. In the relativistic work, these lines slope less than in the nonrelativistic work.

A recent measurement of $\mu_I(Pu^{239})$ by Faust, Marrus, and Nierenberg[40] shows that $\mu_I = 0.20$ nm. A vertical broken line in Fig. 10 represents the value of Ω for this μ_I and F = 1. If all A values were raised by the full 15 Mc/sec uncertainty, the lines could cross at the intercept of this line with the J = 1 line for A < 0. However, the method used to obtain these A values should make the A's for the lower J values much more accurate than those of higher J values (the uncertainty in A for low J might be no more than 10%). Thus, it seems likely that the lines should meet in the region of $\Omega = 14$ or $\Omega = 10$, depending on whether A is less or greater than zero. Such a meeting would correspond to multiplying the relativistic radial integrals by F = 0.74 or 0.55 for $\Omega = 14$ and 10, respectively. The ratio of $\langle 1/r^3 \rangle$ obtained from the spin-orbit constant to the relativistic $\langle 1/r^3 \rangle$ is 0.76, which agrees well with the former number (0.04). If our assumption that the A's for J = 2, 3, 4 are well known is correct, this would seem to indicate that A(Pu) is less than zero; if it is incorrect, there is still reason to believe that F = 0.75 could be the intersection point. Because of the slight slope of the J = 1 line, however, the amount of core polarization does not vary much between the values of Ω corresponding to F = 0.75 and F = 1.0. The value is approximately

$$\Delta A(Pu) = -2, \ -12 \text{ Mc/sec},$$

depending on whether A(Pu) is positive or negative. Defining the crossing point in the graph given by Bauche and Judd[8] as the point on the J = 1 line corresponding to $\mu_I = 0.20$ nm, one obtains

$$\Delta A = -14, \ -28 \text{ Mc/sec}.$$

From Eq. (69), we see that, assuming that the energy levels of the 5f, 7s, and s' electrons and the eigenfunctions $\psi_{7s}(0)$ and

$\psi_{s'}(0)$ are the same for Pu and Am,

$$\frac{\Delta A(\mathrm{Am})}{\Delta A(\mathrm{Pu})} = \frac{(g_J(\mathrm{Am}) + 1)\,\mu_I(\mathrm{Am})\,I(\mathrm{Pu})}{(g_J(\mathrm{Pu}) + 1)\,\mu_I(\mathrm{Pu})\,I(\mathrm{Am})}$$

$$\Delta A(\mathrm{Am}^{241}) = 3.2\ \Delta A(\mathrm{Pu})$$

$$\Delta A(\mathrm{Am}^{242}) = 1.9\ \Delta A(\mathrm{Pu})$$

or

$$\Delta A(\mathrm{Am}^{241}) = -6.5,\ -39\ \mathrm{Mc/sec}$$
$$\Delta A(\mathrm{Am}^{242}) = -4,\ -23\ \mathrm{Mc/sec},$$

the choice depending on the sign of A for the J = 1 state of Pu. These numbers are consistent with those obtained above for ΔA if the A's of Am and Pu both have the same sign.

The value of B is calculated on the basis of Eq. (56). The angular matrix elements are given in Table XI. The following 9-j symbols were required in the calculation:

$$\begin{Bmatrix} 5/2 & 5/2 & 1 \\ 1 & 2 & 1 \\ 7/2 & 7/2 & 2 \end{Bmatrix} = -\frac{1}{2^2 \cdot 3 \cdot 7}\sqrt{3/5}$$

$$\begin{Bmatrix} 5/2 & 5/2 & 1 \\ 1 & 2 & 3 \\ 7/2 & 7/2 & 2 \end{Bmatrix} = \frac{19}{2^2 \cdot 3^2 \cdot 7^2}\sqrt{3/5}$$

The radial integrals are given in Table VIII and the various contributions to Z^2 in Table XII. The final result is

$$B = 0.120\,\frac{e^2 Q}{a_0^3} \qquad (98)$$
$$= 28.2\ Q\ \mathrm{Mc/sec}.$$

Table XI. Angular matrix elements of quadrupole interaction.

$\langle f^7\ {}^6P \| W^{13} \| f^7\ {}^6D \rangle = 3\sqrt{2}$
$\langle f^7\ {}^6P \| W^{02} \| f^7\ {}^6D \rangle = \sqrt{45/14}$
$\langle f^7\ {}^6P \| W^{11} \| f^7\ {}^6D \rangle = -9/2(\sqrt{2/3})$
$\langle f^7\ {}^8S \| W^{11} \| f^7\ {}^6P \rangle = 2\sqrt{6}$

Table XII. Matrix elements of Z^2.

	R_{++}	R_{+-}	R_{--}
$\langle {}^8S_{7/2} \| Z^2 \| {}^6P_{7/2} \rangle$	$8/49(\sqrt{15})$	$-\ 24/245(\sqrt{15})$	$-\ 16/245(\sqrt{15})$
$\langle {}^6P_{7/2} \| Z^2 \| {}^6D_{7/2} \rangle$	$-\ 250/3\cdot 7^3(\sqrt{6/7})$	$-\ 1784/3\cdot 5\cdot 7^3(\sqrt{6/7})$	$-\ 396/3\cdot 5\cdot 7^3(\sqrt{6/7})$

Since the measured quadrupole moment of Am^{241} is +4.9 barns,[41] B(241) is predicted positive, which forces A(241) to be negative. As positive B and negative A are consistent with all of the above results, we believe that this is a true representation of their signs. If it is, then both A(242) and B(242) are negative.

Contributions to A and B from relativistic and other effects are tabulated in Table XIII.

Comparison of Eq. (98) with the measured B values would then give

$$Q(241) = 4.4 \text{ barns}$$

$$Q(242) = -2.5 \text{ barns.}$$

E. Nuclear Structure

Fred and Tomkins,[42] on the basis of spectrum analysis, determined the spin of Am^{241} to be $I = 5/2$. After investigating the α decay of Am^{241} to Np^{237}, Stephens, Asaro, and Perlman[43] concluded that the unpaired 95th proton must be in the Nilsson orbital 5/2-[523]. This assignment fits the Nilsson energy-level diagram exactly if $0.21 < \delta < 0.28$. One can also obtain a value for the deformation from the optically measured quadrupole moment $Q = 4.9$ barns,[41] using Eqs. (94) and (95); the derived value of $\delta = 0.21$ supports the proposed orbital assignment of protons.

The magnetic moment μ_I of Am^{241} has been calculated on the basis of the Nilsson wavefunctions. Table XIV shows the results of this calculation, which was performed for several positive values of δ with both free nucleon g factors and quenched g factors.[32] The value $g_R = Z/A$ was used. We see that, when free nucleon g factors are used, the measured moment is predicted for $\delta \approx 0.15$; with quenched g factors, δ is predicted for slightly greater than 0.2. Because the result with quenched g factors is consistent with that previously obtained, we believe that the use of quenched g factors in calculations concerning Am^{241} is justified.

In Am^{242}, the odd neutron is probably in the Nilsson orbit 5/2+[622]. This assignment, which corresponds to $0.22 < \delta < 0.26$, is also made for the odd neutron in the ground states of the isotones

Table XIII. Contributions to the hyperfine constants A and B in americium.

	Magnitude	
	A (Mc/sec)	B (Mc/sec)
Breakdown of LS coupling within $(5f)^7(7s)^2$	$26.4 \frac{\mu_I}{I}$ [a]	$27.9\ Q$ [b]
Relativistic corrections	$28.5 \frac{\mu_I}{I}$	$0.3\ Q$
Core polarization	$-81.6 \frac{\mu_I}{I}$	0
Total calculated	$-26.7 \frac{\mu_I}{I}$	$28.2\ Q$
Total measured	$-26.7 \frac{\mu_I}{I}$	$25.3\ Q$

a. μ_I in nm.
b. Q in barns.

Table XIV. Am^{241} nuclear moments calculated with Nilsson wavefunctions.[a]

	η		
	2	4	6
Free-nucleon g factors	1.89	1.32	1.07
Quenched g factors	1.95	1.58	1.41

a. Proton state 5/2 -[523].

Pu^{241} and Cm^{243}. Using the coupling rules of Gallagher and Moszkowski,[13] we then have $K = \Omega_P - \Omega_N = 0$ for Am^{242}. For a $K = 0$ nucleus, $\mu_I = g_R I$; if we accept the proposed value of K, we then have a direct measurement of the core g factor. The measured value of g_R, or μ_I, is 0.381, to be compared to the usually used value of $g_R = Z/A = 0.392$.

Because $K = 0$, we have

$$Q = -\frac{1}{5} Q_0.$$

Using the Q obtained in the preceding section, we have $Q_0 = 12.5$ barns. This is of the proper sign and magnitude [$Q_0(241) = 13.5$ barns] for a nuclide in this region.

ACKNOWLEDGMENTS

I thank the many people involved in bringing this research to a successful conclusion, especially:

Professor William A. Nierenberg for his support,

Professor Richard Marrus for his constant help and encouragement,

Eldred Calhoon of the Health Chemistry monitors for his valuable aid in handling radioactive samples,

Douglas B. Macdonald for his engineering aid,

Miss Christina Frank for typing the original version of the manuscript, and

My psychologist.

This research was supported by the U. S. Atomic Energy Commission.

REFERENCES

1. Lloyd Armstrong, Jr., and Richard Marrus, Phys. Rev. 138, B310 (1965).
2. N. F. Ramsey, Molecular Beams (Oxford University Press, London, 1956).
3. E. Fermi, Z. Physik 60, 320 (1930).
4. C. Schwartz, Phys. Rev. 97, 380 (1955).
5. G. Breit, Nature 122, 649 (1928); H. Margenau, Phys. Rev. 57, 383 (1940).
6. P. G. H. Sandars and G. K. Woodgate, Proc. Roy. Soc. (London) A257, 269 (1960); V. Heine, Phys. Rev. 107, 1002 (1957).
7. M. Cohen, D. A. Goodings, and V. Heine, Proc. Phys. Soc. (London) 73, 811 (1959).
8. J. Bauche and B. R. Judd, Proc. Phys. Soc. (London) 83, 145 (1964).
9. K. Rajnak and B. G. Wybourne, Phys. Rev. 132, 280 (1963).
10. A. Bohr and V. F. Weisskopf, Phys. Rev. 77, 94 (1950).
11. J. E. Rosenthal and G. Breit, Phys. Rev. 41, 429 (1932).
12. S. G. Nilsson, Kgl. Danske Videnskab. Selskab, Mat-Fys. Medd. 29, No. 16 (1955).
13. C. J. Gallagher, Jr., and S. A. Moszkowski, Phys. Rev. 111, 1282 (1958).
14. W. A. Nierenberg and G. O. Brink, J. Phys. Radium 19, 816 (1958); P. G. H. Sandars and G. K. Woodgate, Nature 181, 1395 (1958).
15. M. B. White, Hyperfine Structures and Nuclear Moments of Lu^{176m}, Br^{80}, Br^{80m}, and I^{132} (Ph. D. Thesis), UCRL-10321, September 1962.
16. R. G. Schlecht, Hyperfine Structures and Anomaly of Li^6 and Li^7 and the Hyperfine Structures of Re^{186} and Re^{188} (Ph. D. Thesis), UCRL-11047, October 1963.
17. R. G. Schlecht, M. B. White, D. W. McColm, Phys. Rev. 138, B306 (1965).

18. R. H. Trees, Phys. Rev. 112, 165 (1958).

19. D. Strominger, J. M. Hollander, and G. T. Seaborg, Rev. Mod. Phys. 30, 585 (1958).

20. R. Winkler, Naturwissenschaften 10, 236 (1964).

21. Hans Kopferman, Nuclear Moments, English version by E. E. Schneider (Academic Press, New York, 1958).

22. Charlotte E. Moore, Atomic Energy Levels (National Bureau of Standards, Washington, D. C., 1958), Vol. III, NBS-467.

23. F. Bloch and A. Siegert, Phys. Rev. 57, 522 (1940).

24. E. U. Condon and G. H. Shortley, Theory of Atomic Structure (Cambridge University Press, Cambridge, England, 1957).

25. Stanley Cohen, Relativistic Self-Consistent Calculation for the Normal Tungsten Atom, UCRL-8634, 1959; Relativistic Self-Consistent Calculation for the Normal Platinum Atom, UCRL-8635, 1959.

26. H. Schuler and H. Korsching, Z. Physik 105, 168 (1937).

27. R. M. Sternheimer, Phys. Rev. 80, 102 (1950); 84, 244 (1951); 95, 736 (1954); 105, 158 (1957).

28. H. B. G. Casimir, On the Interaction Between Atomic Nuclei and Electrons (Teyler's Tweede Genootschap, Haarlem, 1936).

29. C. Schwartz, Phys. Rev. 105, 173 (1957).

30. Quoted by B. Bleaney as private communication from P. G. H. Sandars (1964).

31. B. R. Mottelson and S. G. Nilsson, Kgl. Danske Videnskab. Selskab, Mat-Fys. Skrifter 1, No. 8 (1959).

32. J. O. Rasmussen and L. W. Chiao, in Proceedings of the International Conference on Nuclear Structure, Kingston, edited by D. A. Bromley and E. W. Vogt (University of Toronto Press, Toronto, Canada, 1960), p. 646; Lung-wen Chiao, The Magnetic Properties of Deformed Nuclei, UCRL-9648, 1961.

33. R. Marrus, W. A. Nierenberg, and J. Winocur, Phys. Rev. 120, 1429 (1960).

34. Joseph Winocur, Some Nuclear and Electronic Ground-State Properties of Pa^{233}, Am^{241}, and 16-hr Am^{242} (Ph. D. Thesis), UCRL-9174, April 1963.

35. M. Fred and F. S. Tomkins, J. Opt. Soc. Am. 47, 1076 (1957).

36. G. Racah, Phys. Rev. 62, 438 (1942); 63, 367 (1943); 76, 1352 (1949).

37. D. Lieberman, J. T. Waber, and D. T. Cromer, (Los Alamos Scientific Laboratory, 1965) private communication.

38. M. Blume, A. J. Freeman, and R. E. Watson, Phys. Rev. 134, A320 (1964).

39. M. E. Foglio and M. H. L. Pryce, Mol. Phys. 4, 287 (1961).

40. J. Faust, R. Marrus, and W. A. Nierenberg, Phys. Letters 16, 71 (1965).

41. T. E. Manning, M. Fred, F. S. Tomkins, Phys. Rev. 102, 1108 (1956).

42. M. Fred and F. S. Tomkins, Phys. Rev. 89, 318 (1953).

43. F. S. Stephens, Frank Asaro, and I. Perlman, Phys. Rev. 113, 212 (1959).

This report was prepared as an account of Government sponsored work. Neither the United States, nor the Commission, nor any person acting on behalf of the Commission:

A. Makes any warranty or representation, expressed or implied, with respect to the accuracy, completeness, or usefulness of the information contained in this report, or that the use of any information, apparatus, method, or process disclosed in this report may not infringe privately owned rights; or

B. Assumes any liabilities with respect to the use of, or for damages resulting from the use of any information, apparatus, method, or process disclosed in this report.

As used in the above, "person acting on behalf of the Commission" includes any employee or contractor of the Commission, or employee of such contractor, to the extent that such employee or contractor of the Commission, or employee of such contractor prepares, disseminates, or provides access to, any information pursuant to his employment or contract with the Commission, or his employment with such contractor.